climate changes spatial planning

Climate scenarios

Soil moisture and root water uptake in climate models

J.C. van Dam | K. Metselaar | L. Wipfler
R.A. Feddes | E. van Meijgaard | B. van den Hurk

KvR 017/11

Soil moisture and root water uptake in climate models

Authors

J.C. van Dam [1]
K. Metselaar [1]
L. Wipfler [1]
R.A. Feddes [1]
E. van Meijgaard [2]
B. van den Hurk [2]

1 Soil Physics, Ecohydrology and Groundwater Management Group, Wageningen UR
2 Royal Netherlands Meteorological Institute

Royal Netherlands
Meteorological Institute
Ministry of Infrastructure and the Environment

KvR report number KvR 017/11
ISBN ISBN/EAN 978-90-8815-012-8

This project (KvR project CS3; Representation of soil moisture and root water uptake in climate models) was carried out in the framework of the Dutch National Research Programme Climate *changes* Spatial Planning. This research programme is co-financed by the Ministry of Infrastructure and the Environment.

Contents

Summary

Summary in Dutch

Nauwkeuriger simulatie van de energie- en waterbalans aan het aardoppervlak is belangrijk om de kwaliteit van regionale klimaatmodellen te verbeteren. We gebruikten een gedetailleerd ecohydrologisch model om vegetatie- en bodemfactoren te rangschikken met betrekking tot hun belang voor modellering van verdamping. De resultaten laten zien dat het type onderrandvoorwaarde, de diepte van de wortelzone, en het temporele verloop van de bladoppervlakte-index de grootste invloed hebben op de jaarlijkse en maandelijkse verdamping. Bodemtextuurdata van de WISE database in combinatie met HYPRESS pedotransferfuncties kunnen worden gebruikt om nauwkeuriger bodemretentie- en doorlatendheidsfuncties af te leiden van het Mualem-van Genuchten type. We voegden recente worteldichtheidsgegevens van agrarische gewassen toe aan de worteldatabase van Schenk and Jackson. We testten de HTESSEL bodemroutine van het regionale klimaatmodel RACMO voor West Hongarije, een gebied waarvoor systematisch een te lage verdamping en te hoge luchttemperatuur wordt berekend met de huidige regionale klimaatmodellen. Satelliet remote sensing gegevens, in combinatie met het SEBAL algoritme, werden gebruikt om verdampingsfluxen af te leiden voor een grid van 1x1 km in het jaar 2005. Vergeleken met satellietgegevens onderschat HTESSEL de verdampingsfluxen enigszins. Dit was vooral het geval in gebieden met irrigatie en ondiep grondwater, factoren die niet zijn opgenomen in HTESSEL. Testen met andere reductiefuncties voor wortelvochtopname, meer realistische bodemdiepte en een concept voor grondwaterinvloed, resulteerden niet in nauwkeuriger ruimtelijk verdeelde verdampingsfluxen in West Hongarije.

Summary

More accurate simulation of the energy and water balance near the Earth surface is important to improve the performance of regional climate models. We used a detailed ecohydrological model to rank the importance of vegetation and soil factors with respect to evapotranspiration modeling. The results show that type of lower boundary condition, root zone depth, and temporal course of leaf area index have the strongest effect on yearly and monthly evapotranspiration. Soil texture data from the WISE database in combination with HYPRESS pedotransferfunctions can be used to derive more accurate Mualem-van Genuchten type soil moisture retention and hydraulic conductivity functions. We added recent literature data on root densities of agricultural crops to the root data base of Schenk and Jackson. We tested the HTESSEL land routine of the regional climate model RACMO for Western Hungary, which shows systematically too low evapotranspiration and too high air temperatures in many numerical regional climate studies. Satellite remote sensing data, in combination with the SEBAL algorithm, were used to derive evapotranspiration fluxes at a 1x1 km grid for the year 2005. Compared to satellite data, HTESSEL somewhat underestimated evapotranspiration fluxes. This underestimation occurred mainly in regions with irrigation and shallow groundwater, factors which are not included in HTESSEL. Tests with other reduction functions for root water uptake, more realistic soil depth, and a concept for groundwater influence did not yield more accurate spatially distributed evapotranspiration fluxes for Western Hungary.

Extended summary

Interactions between atmosphere and land surface affect the energy and water balance near the Earth surface. Although extensive knowledge exists of the physics and nature of these interactions, it's simulation in regional and global climate models is still problematic. One main problem is the limited availability of required input data of vegetation, soils, and drainage. Another main problem is that most soil surface data have a much smaller scale (typical plot or field level) than the much larger scale applied in climate models. In order to improve existing landroutines in current climate models, detailed physical descriptions were confronted with restricted data-availability and data-representivity. Especially the land routines TESSEL and it's successor HTESSEL received attention. Both landroutines are part of the regional climate model RACMO, which is used by the Royal Netherlands Meteorological Institute (KNMI). In KvR project CS3 the following research packages have been performed:

1. Ranking the importance of vegetation and soil factors;
2. Description of European soil variability;
3. Overview of agricultural crop root distributions;
4. Evaluation of the land surface scheme HTESSEL.

In this final report the main objectives, methodologies and results of these four research packages are summarized.

In order to rank the importance of vegetation and soil factors, a simulation experiment has been designed and performed with the Soil Water Atmosphere Plant (SWAP) model. In this experiment the main water balance effects of individual factors were derived given simultaneous variation in all other factors. The ranking of the variables in terms of their relative effect suggests a priority in the processes to be incorporated in new climate land routines. Based on expert judgment, 13 factors were selected: leaf area index and its time course, rooting depth and its time course, soil profile discretisation, analytical function of the soil hydraulic properties, stoniness, the transpiration reduction function with respect to soil moisture, the critical soil water pressure head, and the lower boundary condition of the soil. Results show that choice of the lower boundary condition, rooting depth, and temporal course of leaf area index have the strongest effect on yearly and monthly evapotranspiration.

In the second research package, European soil variability and available methods for its representation were reviewed. We matched processes already available in more extensive hydrological models as well as available soil information. The results suggest that considerable scope exists for adding relevant soil information. The following physical factors may be added: soil depth, soil salinity, soil texture, soil stoniness and groundwater levels. Soil depth, soil salinity, soil texture and soil stoniness are part of the WISE database. Soil texture data can be used to generate more accurate soil moisture retention and hydraulic conductivity functions, using the HYPRESS database. The FAO-drainage classification can be used with the soil depth, slope class, and texture information to generate input for a groundwater submodule. A concept has been formulated to translate drainage classes of The Netherlands into the FAO drainage classes. This concept requires further validation.

Soil root density profiles play a key role in plant transpiration and thus the sensible heat flux. We employed the root data base of Schenk and Jackson (2002) and added recent literature data on root densities of agricultural crops. We tested 4 analytical functions to describe the root data and selected the logistic dose-response function as most suitable function. For this function we calibrated the input parameters for the main vegetation types. These data can be used in both macroscopic and microscopic root water uptake models. We also analyzed whether a correlation exists between root

density distribution parameters of agricultural crops and climate as well as management factors. This correlation was not significant. For specific cases we showed that root density distribution parameters are not constant with time, but we are far from a predictive relationship. Therefore at present root density distributions for agricultural crops are described with constant parameters.

In the last research package, the skill of the land surface model HTESSEL was assessed to reproduce evaporation in response to spatial variable land surface characteristics and atmospheric forcing. A problem often reported in numerical regional climate studies is a systematic summer drying, that results in too dry and too warm simulations of summertime climate in south-eastern Europe. We obtained satellite evapotranspiration data for the 2005 growing season in the Western part of Hungary and compared these to HTESSEL model results. Atmospheric forcing was obtained from a hind cast run with the regional climate model RACMO. Although HTESSEL slightly underestimated the seasonal evaporative fraction as compared to satellite estimates, the mean, 10th and 90th percentile of this variable were of the same magnitude as the satellite observations. The initial water as stored in the soil and snow layer did not have a significant effect on the statistical properties of the evaporative fraction. However, the spatial distribution of the initial soil and snow water affected significantly the spatial distribution of the calculated evaporative fraction and the model ability to reproduce evaporation correctly in low precipitation areas. HTESSEL's performance appears to be less in more dry areas. In Western Hungary these areas are situated in the Danube valley, which is partly covered by irrigated cropland and which also may be affected by shallow groundwater. Incorporating groundwater influence and irrigation application, processes that were not included, may improve HTESSEL's ability to predict evaporation correctly.

Based on our sensitivity analysis, the effect of a number of modifications to HTESSEL was assessed. A more physically based reduction function for dry soils was introduced, the soil depth was made variable and the effect of shallow groundwater was included. For Hungary and the year 2005, these modifications did not lead to a better performance of HTESSEL. The more physically based root water uptake reduction function increased the evapotranspiration too much. The decreased soil depth resulted in too low evapotranspiration. The modification of the soil moisture characteristic was insufficient to explain the larger evapotranspiration in areas with shallow groundwater levels. Integrated model runs on European scale for larger time frames should reveal the real merit of these modifications.

The Synthesis Chapter 6 contains recent scientific literature on land surface schemes in climate models. In this context the contribution of our research findings are described with respect to the relevance of soil moisture modeling, the current performance of the HTESSEL land surface scheme, the inclusion of groundwater and irrigation, and the availability of input and verification data.

1. Introduction

Background

Natural hydrological systems are presently seriously affected by changes in land use and climate, resulting in landscape degradation, river and groundwater pollution, and increasing effects of floods, droughts and salinisation. Soil-vegetation-atmosphere interactions determine to a large extent the climate and the behaviour of the hydrological cycle. Studies with different climate models showed that vegetation and other land surface properties directly affect regional climate. Such impacts may lead to geographically remote changes in temperature and precipitation via atmospheric circulations. Soil moisture in atmospheric models controls the partitioning of available energy into latent (evapotranspiration) and sensible heat and thus represents a central element in reliable climate modelling. Therefore soil moisture forms the key to more accurate prediction of near surface temperature and humidity in climate and weather-prediction models.

Representation problems of soil moisture at different scales

Given the spatial scales implicit in climate models any notion of an observable soil moisture, or an "average" soil moisture is problematic. A gap therefore exists between what climate modellers mean by soil moisture and what experimentalists mean by the same term. This hinders our efforts to improve models of large scale soil moisture. Modellers need a soil moisture definition which can be used in a hierarchy of models and which can be translated into an observable quantity. In addition, land surface modellers want to compare their simulations to observed soil moisture, which is only possible if the modelled and observed soil moisture are representative of similar spatial scales. Observed soil moisture representative at a point cannot directly be compared to soil moisture simulated by a land-surface scheme. One key product needed by the climate community is a clear conversion of climate-model soil moisture into measurable soil moisture.

Problems of land surface parameterization

Regional climate scenario calculations for central Europe suffer from systematic dry summer biases (i.e. underestimation of precipitation) owing to a too small buffering capacity of the soil hydrological reservoir. Pragmatic solutions to this well-known and often reported drift is to increase the soil reservoir depth, which significantly reduces the dry warm biases in continental summer. But it is unclear how realistic these pragmatic solutions are, and whether they are still valid when extrapolating climate simulations to future climate conditions.

Previous land surface parameterization schemes that were applied in RACMO2 failed because of deficiencies in description of the soil hydraulic properties, of the rooting depth and rooting distribution, and improper handling of the lower boundary condition (Lenderink et al, 2003). An additional complication is that numerical weather and climate prediction models need observations for initialization, system parameter calibration and adjustment of forecasts. However, the current European data bases on soil properties, root densities and drainage conditions show a limited suitability for climate modelling.

Surface water balance modelling at large scales

As stated above, there are major difficulties in simulating soil moisture by climate models: various land surface models simulate very different amounts for a given state of the climate. These differences are not believed to affect the reliability of the climate model for simulating the climate, or changes in the climate. The reason is that soil moisture is simulated to provide information for calculating evapotranspiration. Even if a large difference in soil moisture exists between two models, this need not be important provided the parameterisation of evapotranspiration is adjusted. These different representations of soil moisture cause major difficulties, however, in comparing modelled soil moisture with observed soil moisture, or in using model-derived soil moisture in impact studies.

In climate models, run-off is usually modelled in a crude way. There is now an increasing consensus that schemes need to differentiate between a quick infiltration excess component and a slow percolation/drainage component. The latter is usually assumed to occur at a rate defined by the prevailing soil hydraulic conductivity, being often calculated through the soil hydraulic functions. European datasets of soil hydraulic functions at the proper scale must then be made available for several soil texture classes. Given the scarcity of data, however, it is presently very common in climate modelling to ignore variation in soil hydraulic properties with soil depth,.

Local point-/field scale ecological and hydrological modelling

Bottom-up point/field scale models are generally constructed around the plant and its soil-root system, These models regard the root system as a diffuse sink that penetrates each depth layer of soil uniformly, though not necessarily with a constant strength throughout the root zone. Details of the root distribution are specified, multiple vertical soil layers are considered together with the soil hydraulic characteristics that determine water availability to the roots. Root water uptake is then being represented as a sink term that is included in the vertical soil water flow equation. To obtain a solution of this flow equation one has to supplement it with conditions for the initial situation and for the top and bottom boundary of the flow system. Based on these principles a group of scientists in Wageningen have developed the vertical Soil-Water-Atmosphere-Plant (SWAP) model (Kroes et al., 2008). This model simulates the water flow, solute transport and heat flow in homogenous as well as heterogeneous layered soils. The model is very flexible in handling different boundary conditions at cropped and bare soil surfaces as well as at the bottom of the soil profile. The model has been tested under very different field conditions and is presently used in more than 70 countries for a variety of different applications (Van Dam et al., 2008). SWAP is producing all the terms of the soil water balance: Actual Transpiration, Actual Soil Evaporation, Infiltration, Soil moisture Storage Change, Percolation and Capillary rise. The idea now is to consider the SWAP-model as the basic 'true' model against which Soil-Vegetation-Atmosphere-Transfer (SVAT) schemes, that are currently in use in regional climate models, can be both tested off line and optimized under different climate forcings. In addition validation will be performed by employing evapotranspiration as measured by satellites at large problematic areas.

The innovation of the approach proposed here is that rather complete physical descriptions are confronted with restricting data-availability and data-representivity, leading finally to SVAT schematisations that will produce the best possible soil water balances. In the frame of this main objective the BSIK project CS3 has been formulated: Representation of soil moisture and root water uptake in climate models. In this project the following research packages have been performed:

1. Ranking the importance of vegetation and soil factors;
2. Description of European soil variability;
3. Overview of agricultural crop root distributions;
4. Evaluation of the land surface scheme HTESSEL.

The methodology and results of these four research packages have been reported in a number of documents, articles and presentations, as listed in the Annex. This final report summarizes the main objectives, methodologies and results of BSIK project CS3. Above four research packages are discussed one by one in the next chapters. The final chapter synthesizes our research findings with recent international scientific studies.

2. Sensitivity of soil hydraulic factors[1]

2.1 Introduction

In literature two main approaches exist to develop and improve models:

1. Model elimination: formulate different models or submodels, test them predictively, and continue with the best predictor (e.g. de Wit et al, 1970; Sinclair and de Wit, 1976). In model elimination one needs to establish that prediction errors between models are significantly different.
2. Model evolution: for a given model, analyze its prediction errors, and, based on an analysis of the causes, reformulate the model (e.g. Beck, 1985). In model evolution one needs to establish that (part of) the prediction errors are indeed systematic.

The case in which a group of models is compared in terms of predictive quality, and the predictive quality of this model group as a whole has to be improved, has not been studied at all. Yet this is the situation SVAT modellers face. As different model intercomparison experiments (PILPS, 2006) have shown, establishing common causes for the predictive error of different models with similar complexity, is far from trivial. Procedures to establish common causes for prediction errors are weakly developed: presently conclusions of expert discussions direct the improvement agenda.

If we return to the case of a single SVAT model, an intermediate step in the elimination approach may be to prioritize different processes in a model in terms of the sensitivity of the model output to these processes. Determining relative importance of processes may offer guidance in model simplification, but also in increasing model complexity. When simplifying a model, one would remove or simplify processes which have a low sensitivity. When increasing complexity, one may

1 Based on Metselaar K., J.C. van Dam & R. A. Feddes, 2006a. Screening and understanding the importance of soil hydrology related factors in a SVAT scheme. Part 1: Screening factors to establish the relative importance. Part 2: A study of numerical discretization, rooting depth, and bottom boundary condition. Reports in the Framework of the KvR project CS3.

decide to test different descriptions of the process to which the relevant output is most sensitive. Alternatively, one may develop increasingly complex versions of the model, sequentially including additional processes ranked in terms of decreasing sensitivity.

In this Chapter we will consider the case of two models (TESSEL and SWAP) which differ in number and detail of processes included. SWAP is the most comprehensive model of the two. Sensitivity analysis of the SWAP model will be used to select processes which may improve TESSEL.

2.2 The SVAT models TESSEL and SWAP

TESSEL

TESSEL is a version of the SVAT-scheme of the European Centre for Medium Range Weather Forecasts (ECMWF, 2006). TESSEL has been used at KNMI in its regional forecasting model RACMO. The algorithm was used with meteorological forcing variables as input. In its operational settings for Europe, TESSEL has a constant Leaf Area Index (LAI) and a constant rooting depth with a fixed root density profile for each vegetation type. Reduction of potential transpiration is a linear function of soil moisture content. TESSEL uses a single homogeneous soil type corresponding to loam. Richards' equation for soil water flow is solved numerically, for which the profile is divided in four numerical layers. Soil moisture retention and hydraulic conductivity are described by the Hornberger-Clapp functions. At the bottom of the soil profile 'free drainage' is assumed.

SWAP

SWAP (Kroes et al., 2008) is a SVAT scheme developed for use in agrohydrological studies at field scale, and for detailed simulation of hydrologic processes, such as plant transpiration, soil evaporation and soil water percolation. Also SWAP solves Richards' equation numerically, based on an accurate implicit numerical scheme. The soil hydraulic functions are described by the analytical functions of Mualem-van Genuchten. Unlike TESSEL, SWAP allows a large flexibility in operational settings. The model may be used with a variable leaf area index, a variable rooting depth, with layered heterogeneous soils, and hysteretic soil physical characteristics. SWAP is flexible in its numerical layering, partitions evapotranspiration in evaporation and transpiration on the basis of the LAI, and uses a transpiration reduction function which is a linear function of soil water pressure head. In addition, the model allows for a large number of bottom boundary conditions.

2.3 European scale

In SVAT-schemes discrete classes are generally chosen to represent variation. In this study we followed this approach. In terms of vegetation patterns, the main land cover in Europe consists of agricultural areas, forests and semi-natural areas. Land cover with a seasonality in leaf area index occupies between 70 and 75%. The area with changing rooting depths is estimated at 30%.

Soil texture, although predominantly loamy, varies significantly across Europe. More importantly however, other factors, such as soil depth, stoniness, salinity and drainage vary as well. Only half of the area is considered to be well-drained. Table 1 offers an overview of the variation in terms of relative area (Fraters, 1996).

Table 1.
Area (% of total) of aggregated soil units based on the FAO soil map (Fraters, 1996).

	Sand	Loam	Clay	Organic	Total
Well-drained	10	32	2		44.0
Shallow and stony	8.5	21	2		31.5
Imperfectly drained	0.5	8.5	4.5	3	16.5
Arid and saline	-	6.5	1.5		8.0
Total	19	68	10	3	100.0

Therefore it is clear that the operational settings of TESSEL ignore a large amount of the spatial and temporal variability present in Europe. As in any predictive application, the justification of this reduction lies in the predictive quality of the model, not in the close correspondence of its parameterization to existing maps. Therefore, an analysis of the sensitivity of this SVAT scheme to inclusion of additional variability may help to improve it's predictive quality.

This Chapter focuses on the variability present at the European scale and analyzes output at two time scales: yearly and monthly. To ensure that the conclusions are robust with respect to weather variability, the effects are analyzed over a period of 44 years for two distinct locations in Europe.

2.4 Experimental design

Based on this brief description of variability of soil and land cover over Europe, and on the differences between TESSEL and SWAP, we want to estimate the relative effect of each individual variable on relevant state variables. Sensitive variables and processes can be used to improve the TESSEL model formulation.

Variables selected

Table 2 presents an overview of selected variables. The reason for selection is their variability on the scale of interest, existing differences between SWAP and TESSEL, or the possibility to use different values in the model. Most of the parameters selected are based on an existing difference between SWAP and TESSEL (factor numbers 1,2,3,4,5,6).

Table 2.
Variables included in the simulation study.

Variable	Selected settings	Alternative, contrasting settings	Setting selected (if possible)	Factor / number	Factor name
Soil depth	Deep	Shallow	3 and 5 m depth	A	Soil depth
Climate	Hungary (Pannonian)	England (Atlantic)		B	Climate
Numerical layers	Coarse	Fine		1	Discretisation
Soil physical functions	Clapp and Hornberger	van Genuchten		2	Soil physical functions
Leaf area index					
in time	Constant	Function of time		3	*LAI* (time)
Root depth in time	Constant	Function of time		4	Root depth (time)
Maximum root depth	Deep	Shallow		5	Max (root depth)
Argument reduction root water uptake	Soil moisture	Soil matric pressure head		6	Sink term (argument)
Partitioning *E* and *T*	Extinction coefficient high	Extinction coefficient low		7	Partitioning ET_p
Sink term, critical head	High	Low		8	Sink term (critical)
Soil texture	Loam	Sand, clay, organic	Sand	9	Texture
Soil phase	Homogeneous	Stones/salt	Stones	10	Stones
Lower boundary condition	Free drainage	Groundwater/ bedrock	Groundwater	11	Lower boundary condition
Leaf area index	High	Low		12	Max *(LAI)*
Root density with depth	Constant	Function of depth		13	Root density (depth)
Soil profile	Single horizon	Multiple horizons	Single horizon	-	
Hysteresis	No	Yes	No	-	

Variables which vary within SWAP, are the parameter defining the partitioning of evapotranspiration over transpiration and evaporation (7) and the parameter defining the soil water pressure head below which actual transpiration becomes smaller than potential transpiration (8). A variable which has been varied in TESSEL is the soil depth (A). Climate (B), soil texture (9) and soil phase (10), and lower boundary condition (11) are factors which significantly vary within Europe. Additionally, we have included contrasting settings of maximum leaf area index (11) and root density profiles (12).

Screening and experimental design

Screening means establishing the relative importance of a large number of different factors as efficiently as possible. We should select a regression model with the highest descriptive performance. Several techniques are available (Welch et al. 1992; Kleijnen, 1987). We did select a design with two factor levels (Genstat, 2003), which allows estimating main effects only, and has no residual degrees of freedom. Our setup consisted of 13 factors (Table 2) which we executed 4 times: twice to analyze the results for different climates, and twice to include the effect of different soil depths.

Analysis

Values of the response variables and the associated levels are input to an ANalysis Of VAriance (ANOVA), which partitions the total variation in the response variable in variation related to the different factors. The model underlying ANOVA is linear, and given the design of the experiment (2 levels for each factor) it can not be otherwise. The mean sum of squares (MSE) is the sum of squares attributed to the factor divided by the degrees of freedom for that factor. In real-world experiments the MSE of a factor is compared to the mean sum of squares of the residuals (RMSE). The residual mean square is the variability which could not be attributed to any factor, and may be regarded as “noise”. This signal-to-noise ratio (MSE/RMSE) is a measure of the relative importance of the factor. As in simulation studies the importance of different factors does not depend on unknown and uncontrolled factors, the noise term is irrelevant (although it does reflect the quality of the linear model assumed). What is interesting, however, is the effect of a factor relative to the effect of weather (i.e. $MSE_{factor}/MSE_{weather}$). A ratio larger than 1 indicates that changing from one factor level to another has an effect larger than the effect attributed to weather. This would mean that when comparing two sites differing in a specific factor their response variable (averaged over a number of weather periods) would be different, the more so, the larger the ratio $MSE_{factor}/MSE_{weather}$. For each climate, and for each soil depth, the results were analyzed in terms of this ratio. Ranking the factors in terms of this ratio reflects the relative importance when changing one setting to another.

2.5 Analysis results

The results for yearly and monthly evapotranspiration are presented. Ranking should be interpreted as the importance of a variable. This importance is expressed as the effect of its variation on evapotranspiration relative to the simultaneous variation of all other factors. The measure is relative to the effect of meteorological variation, i.e. a value of 100 means that the effect is 100 time stronger than the effect attributed to the meteorological variability.

Yearly evapotranspiration

Figure 1 shows the ranking of the factors in terms of their variance ratio for cumulative yearly evapotranspiration for two soil depths. Most important factors are lower boundary condition, maximum rooting depth and temporal variation of leaf area index *(LAI)*. The ranking was not sensitive to soil depth and climate.

Monthly evapotranspiration

The above analysis also allows establishing sensitivity patterns on shorter time scales. Figure 2a presents the variance ratio for the three most important factors in the Atlantic climate (England) as a function of time. Figure 2b does so for the Pannonian climate (Hungary). Both results are based on the simulations for the soil depth of 3 m.

2.6 Discussion and conclusions

Importance of factors

The ranking of the most important factors seems not sensitive to both climate and soil depth. For the current settings, the lower boundary condition, the maximum rooting depth, and the presence or absence of a temporal variation in *LAI* have the highest ranking. This suggests that analyzing the effect of these parameters on predictive quality is most interesting.

Temporal sensitivity

The result presented in Figure 2 suggests that in specific months (notably after leaf area index has stabilized) analysis of remote sensing images in terms of evapotranspiration may indicate absence or presence of a groundwater level. Interestingly enough, differences in rooting depth may have a similar effect on evapotranspiration.

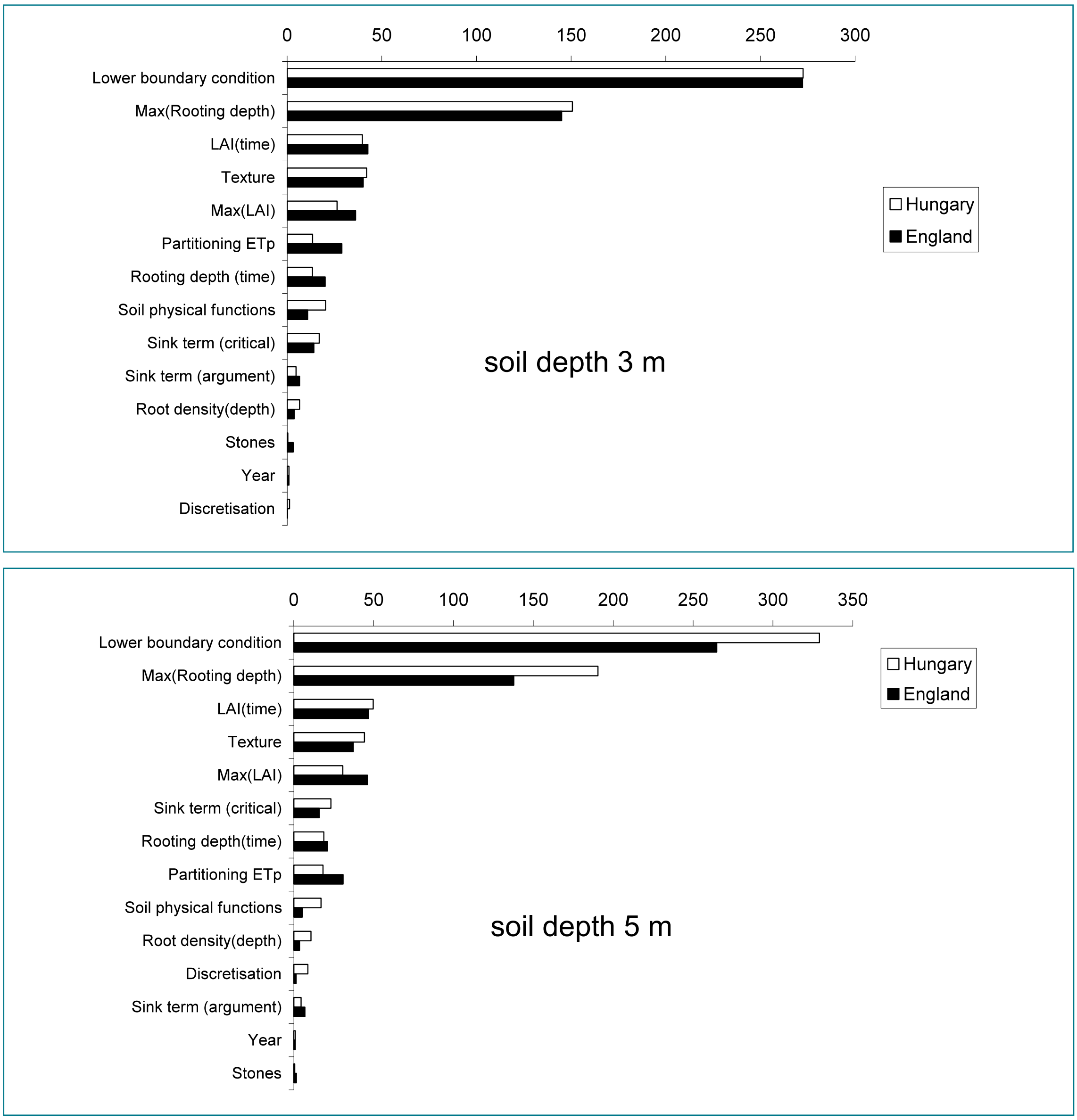

Figure 1. Effects of the different factors on yearly cumulative evapotranspiration for two climates (Pannonian in Hungary and Atlantic in England) and two soil depths. Effects are presented as a variance ratio, i.e. expressed relative to the mean variance of the yearly evapotranspiration.

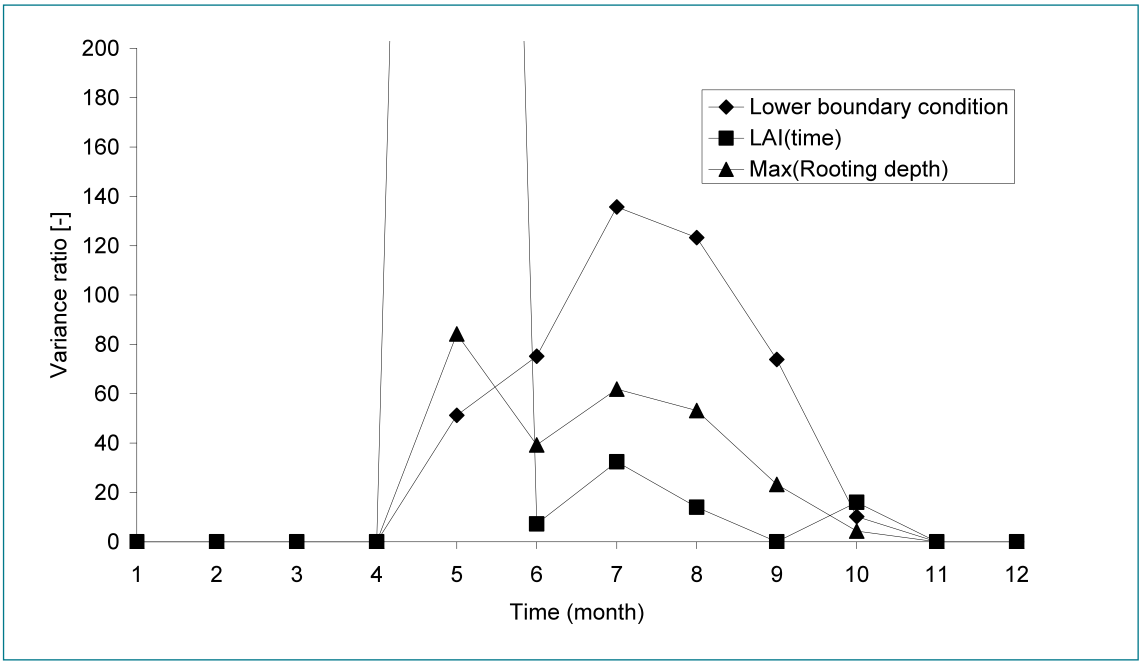

Figure 2a. Variance ratio for lower boundary condition, for time course of leaf area index, and for maximum root depth as a function of time for the Atlantic climate (England) and 3 m soil depth.

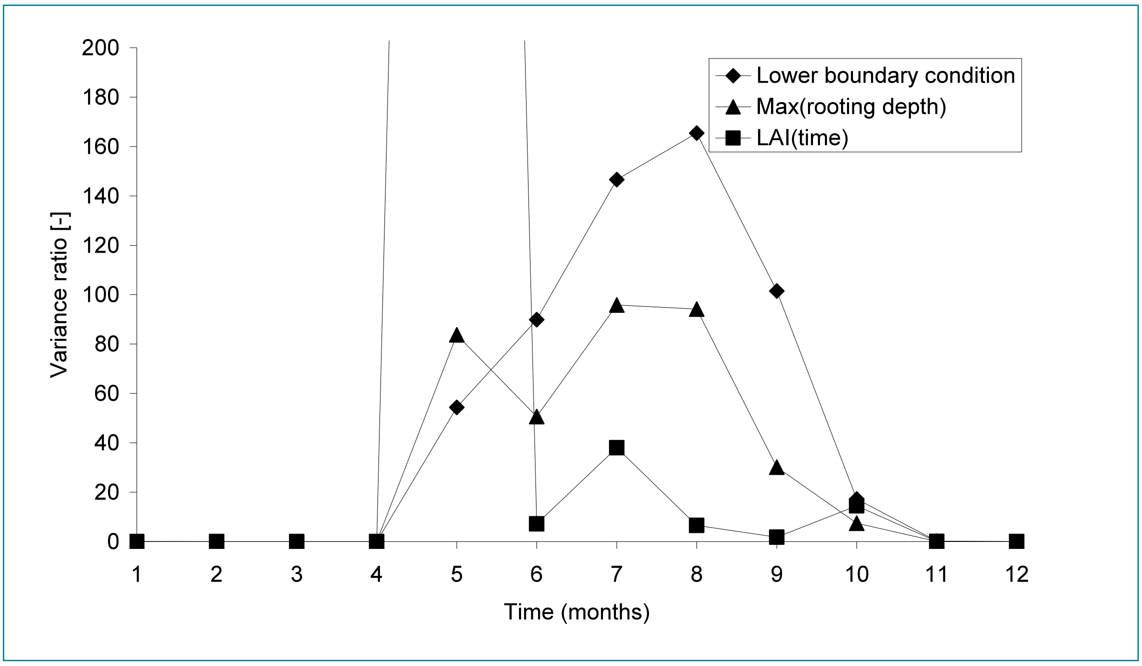

Figure 2b. As Figure 2a, in this case for the Hungarian climate.

Choice of factor settings and intercomparability of factor effects

It should be clear that given the nature of the factors considered, comparability of effects has its limitations. Numerical discretisation and maximum *LAI* are completely different types of variables: *LAI* can be measured over Europe, while discretisation is a model property. Even if the mathematical interpretation of the value would be the same, e.g. the same probability of exceedance, the population from which the value stems (the population of experiments versus a population of models) would be incomparable. The intracomparibility of factors (comparison of factors of the same type - e.g. a comparison of the effects of default model settings) is less problematical, as these values already have the same meaning.

Numerical discretization

In a separate study we investigated the lower boundary condition and maximum rooting depth together with the numerical discretization. Results show that sensitivity to the lower boundary condition and maximum rooting depth decreases with a decreasing number of soil layers. Using a coarse discretization may therefore underestimate their importance. In the presence of a groundwater table, assumptions regarding capillary rise and root water uptake at insufficient aeration become important.

Methodology

Whereas the approach itself is relatively straightforward, both the execution and the analysis of the results are not. Additional software for input file generation and output file analysis was written.

2.7 Summary

In this Chapter a simulation experiment with the ecohydrological model SWAP has been performed. The experiment was set up to derive the main effect of an individual variable on different water balance terms given simultaneous variation in all other factors. The ranking of the variables in terms of their relative effect suggests a priority in the processes to be incorporated in new versions of SVAT scheme such as TESSEL. The experiment was set up to analyze the effects of 13 factors: leaf area index and its time course, root depth and its time course, profile discretisation, description of the soil hydraulic characteristics (Hornberger-Clapp vs. van Genuchten), stoniness, the reduction of vegetation transpiration as a function of moisture content or as a function of soil matric head, the point at which reduction of transpiration occurs, and the lower boundary condition of the soil.

Results show that the choice of the lower boundary condition, the maximum rooting depth, and temporal variability of leaf area index have the strongest effect on yearly and monthly evapotranspiration.

3. Soil variability in Europe[2]

3.1 Introduction

In this Chapter we consider refinement of European soil information for use in meso-scale meteorological models. We will focus on the land routine TESSEL which is used at the KNMI in their meso-scale model RACMO.

In TESSEL the transport equation describing soil moisture flow is solved assuming unit gradient as the bottom boundary, which corresponds to a soil profile which is drained by gravity and no groundwater influence. At present soil properties used in TESSEL are based on soil physical characteristics according to Clapp and Hornberger. The characteristics are parameterized on the basis of averages of tabulated values for US texture classes (silt loam, loam, silty clay and clay

2 Based on Metselaar K., R.A. Feddes & J.C. van Dam, 2006b. Soil variability in Europe, and a quick scan of its parameterization for use in SVAT-schemes. Reports in the Framework of the KvR project CS3.

loam), and represent a medium textured (loamy) soil for entire Europe. The soil is considered to be homogeneous, so no soil horizons are distinguished.

3.2 Soil maps

European soil maps

Figure 3 shows a soil map which gives an impression of the large soil variability in Europe (Stanners and Bourdeau, 1995). Work on the European soil map at scale 1:1,000,000 is ongoing. The European soil bureau (Eusoils, 2006a) coordinates the activities linked to the European soil map.

The soil map and its map units are linked to databases of soil profile characteristics. These can be used to predict soil hydraulic functions or other derived properties. The database contains fields defining soil depth and soil stoniness. Groundwater level, stoniness and salinity are also qualified as a class 'most important limitations to agriculture'. In addition, maps of groundwater resources are digitally available at a scale of 1:500,000. (Eusoils, 2006b). These maps contain groundwater levels, and when significant their yearly fluctuations (Hollis et al., 2002).

Based on the report by Fraters (1996), the relative areas for soil types can be derived (Table 3). Loamy soils dominate the map: they cover 68% of the map area. This explains the choice of a loamy texture in TESSEL. Nevertheless, the soil profile as used in TESSEL (column label 'well-drained', row label 'loamy') is representative for only 32 % of all European soils!

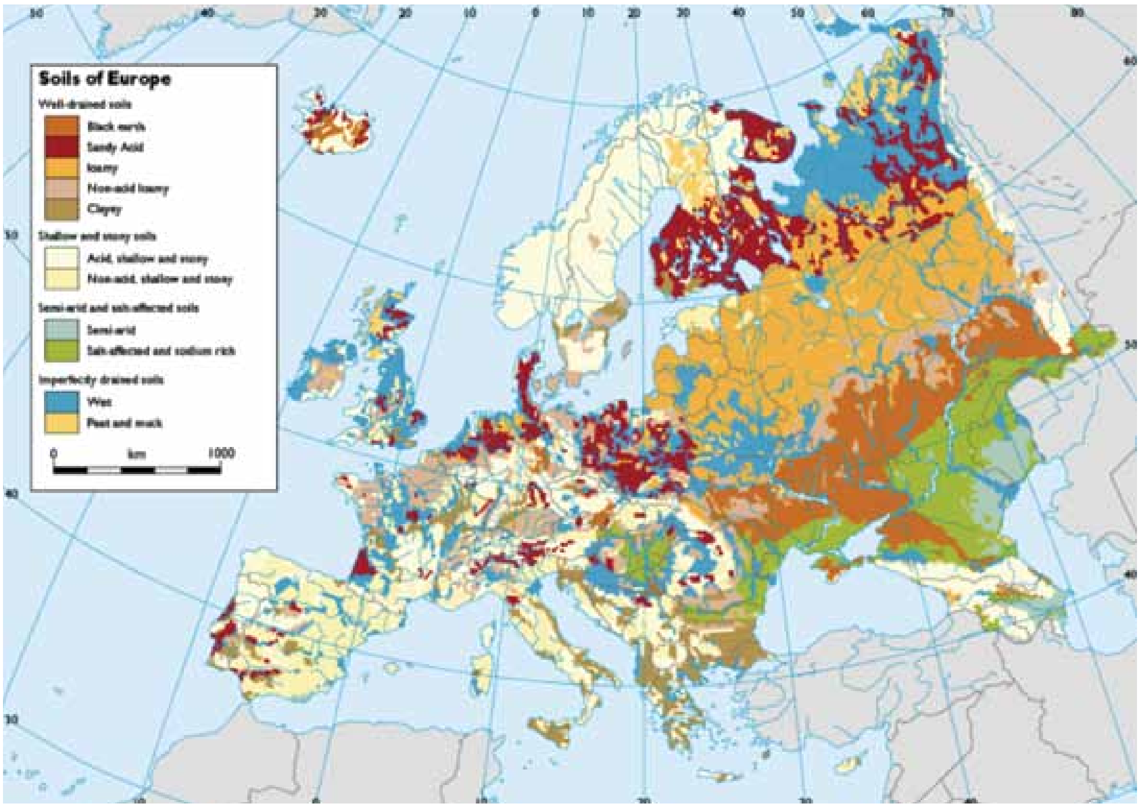

Figure 3. Soil map of Europe, without Turkey (Stanners and Bourdeau, 1995).

Table 3.
Relative areas of soil types (%) in Europe (Fraters, 1996).

% Area	Imperfectly drained	Saline or sodic	Stony 'deep'	Stony 'shallow'	Lithic 'shallow'	Well-drained	Total
Organic	3						3
Sandy	0.5	0	0	8.5	0	10	19
Loamy	8.5	6.5	0	13.5	7.5	32	68
Clayey	4.5	1.5	2	0	0	2	10
Total	16.5	8	2	22	7.5	44	100

3.3 Pedotransfer functions

Soil hydraulic functions

There exists a large number of studies on pedotransfer functions, which link soil hydraulic functions to texture. Two main approaches are followed: those predicting a table with data pairs, and those predicting parameters of analytical functions. A literature review showed that in Europe the most extensive concerted action to establish pedotransfer functions was performed by HYPRES (2006). These pedotransfer functions are part of the European soil database. For global studies Reynolds et al. (2000) used the WISE v1.1 database (Batjes, 2002a) to derive the soil hydraulic functions on the basis of the pedotransfer functions presented by Saxton et al. (1986). The basis for their analysis are Brooks and Corey type soil hydraulic functions.

Nemes et al. (2003) compared national, continental and intercontinental pedotransfer-functions. As the differences in predicted soil moisture contents were small, he suggests that using international pedotransfer functions may be preferable to national functions. Tests of predictive quality remain necessary. An overview of publications of regional, national, and international studies with respect to pedotransfer functions with a European focus is presented in Metselaar et al. (2006b). In European case studies soil hydraulic functions are generally described in terms of the so-called van Genuchten parameters.

Stoniness

Stoniness is an issue in global agro-ecological research (Fischer et al. 2000). However, the tipping bucket type approach used in that analysis only requires a correction of the plant available moisture. As a rule of thumb the available moisture is halved when a stony or petric phase is present. In the WISE v2.1 database volumetric gravel content (fragments > 2 mm) are given, and linked to the legend of the FAO soil map. In this case no additional rules are required.

Salinity

On the basis of the soil map relative area (Fraters, 1996), salinity is an issue in 8% of the European continent, notably in Hungary. Links to the soil map on world scale are provided, as WISE v2.1 contains sodicity and electrical conductivity data. The latter could provide input to simulate reduction of transpiration due to salinization. No additional transfer rules are required.

Soil depth

Taxotransfer rules might be used to determine rooting depth classes. This variable is used in the calculation of the amount of plant available water, but might not reflect the actual soil depth. In the calculation of the available soil moisture in the WISE v2.1 database (Batjes, 2002b) a soil depth of 100 cm is used, except for some soil types in the FAO soil map (Lithosoils: 10 cm; Rankers and Rendzinas: 30 cm). The WISE v2.1 database also contains information on the maximum depth in soil pit descriptions, generally the depth to rock, or the depth without strong physical limitation. Obviously this offers the most straightforward definition of soil depth, and the possibility to set a well-defined bottom boundary condition in modelling. However, it is not clear in which cases maximum depth reflects the depth to groundwater or to the parent material. In this case no additional transfer rules are required.

Drainage

Also drainage classes can be distinguished on the basis of soil classification. The classes are used in the calculation of the rooting depth, and results in modification of the plant available moisture. If the soil is under groundwater influence, available soil moisture is increased. In a study for the Dutch scientific council for government policy (WRR, 1992) drainage classes are linked to the FAO-soil names by taxotransfer rules. Drainage is described in 7 classes from very poorly drained to excessively drained. The transfer rules used to establish drainage classes are presented in Metselaar et al. (2006b). Five of the seven FAO drainage classes allow a groundwater table.

3.4 Groundwater influence

General

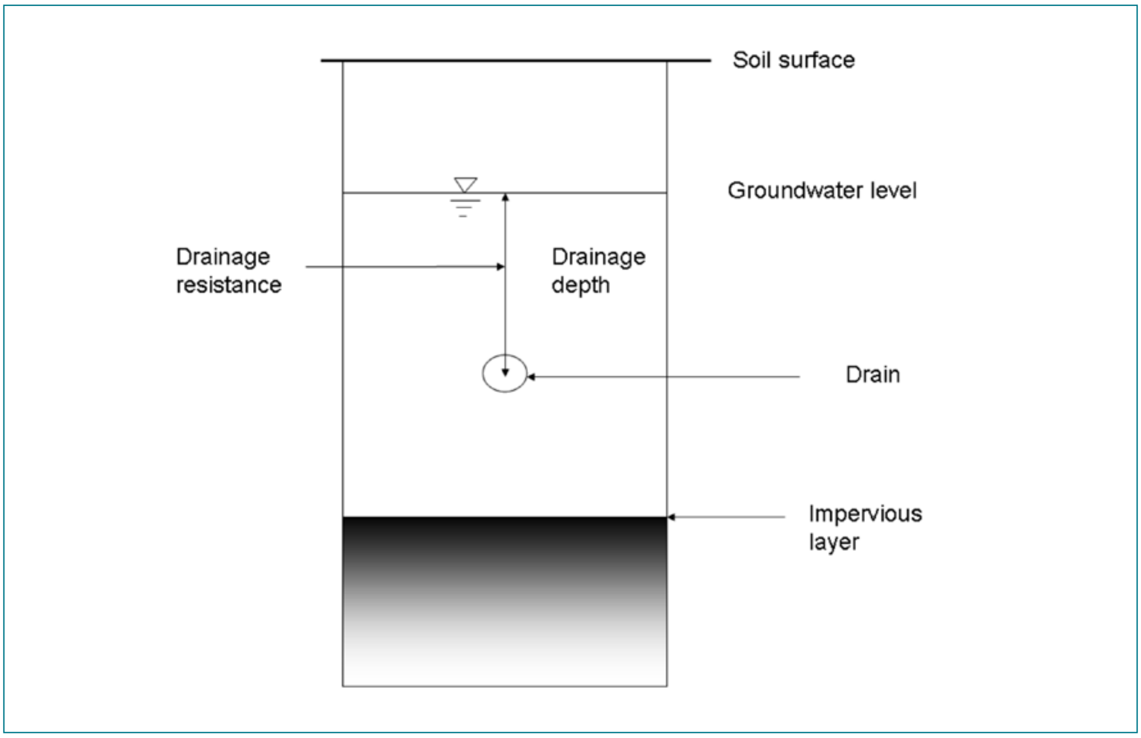

Figure 4.
Soil profile schematization to incorporate drainage and fluctuating groundwater levels.

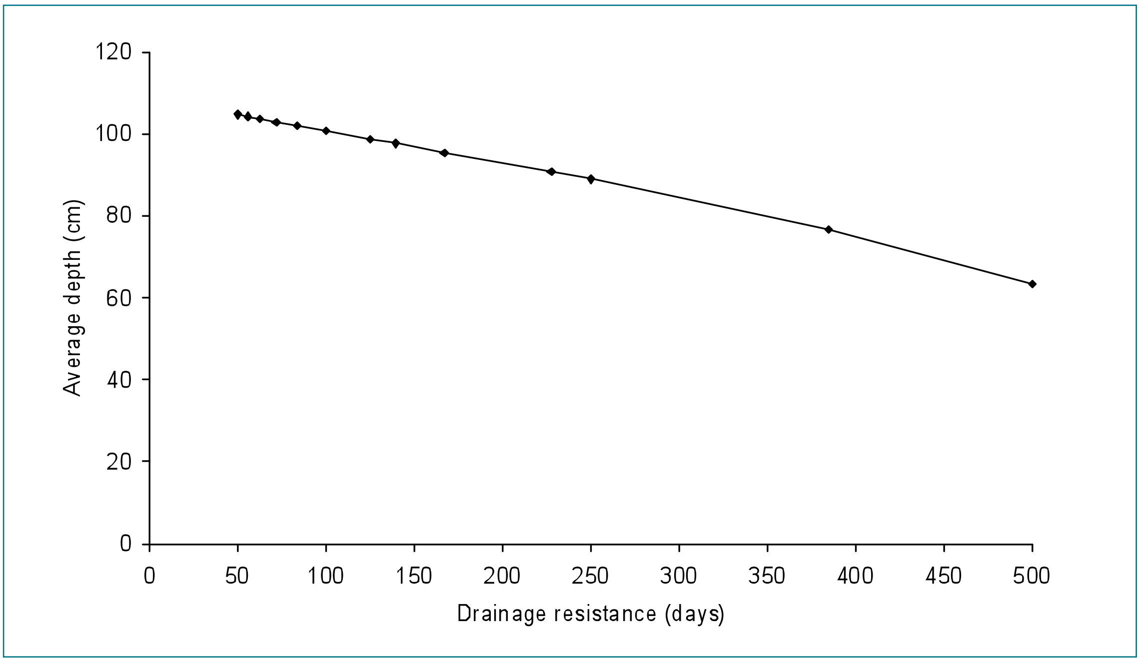

Figure 5a.
Simulated average groundwater depth (yearly) as a function of drainage resistance.

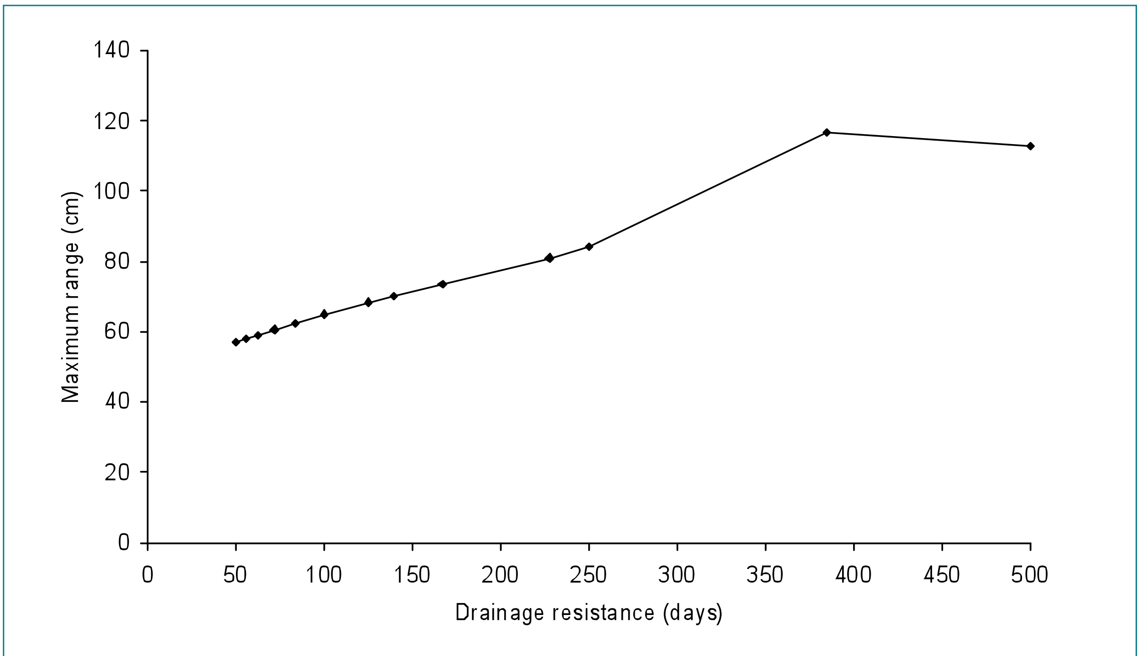

Figure 5b.
Simulated groundwater range as the difference between maximum and minimum level as a function of drainage resistance.

Drainage rate is usually characterized by the drainage resistance, the drainage level and thickness of the aquifer. Figure 4 shows the main characteristics of a soil profile with lateral drainage. Various options to calculate drainage fluxes have been implemented in the SWAP model (Kroes et al., 2008). The simplest option requires the following input: drainage resistance, drainage level, and the impervious layer depth.

An example

Using the drainage parameterization described above, drainage resistance at a drain level of 100 cm was varied in the range 50 - 500 days. The soil texture is homogeneous fine sand. The water balance was simulated for a single year, taking into account an initialization run. The resulting average groundwater depth and the maximum range are shown in Figure 5. A low drainage resistance results in a groundwater level close to the drainage level, and a small maximum range. A low resistance implies a fast response of the drains, and the soil is well-drained. A high resistance results in a groundwater level above the drains, and a large range. The higher the resistance, the slower the response of the drains, and the more poorly drained the soil. Apart from changing the resistance, changing the drainage level will affect the groundwater levels.

The required input (drainage resistance, drainage level, and depth to impervious layer) can be chosen in such a way that the simulated groundwater behaviour matches the FAO drainage class defined for the soil unit. Whereas this is qualitatively possible, the FAO drainage criteria need to be quantified, e.g. what is meant with “at shallow depth”?

Relation between FAO and Dutch groundwater classes

The Dutch groundwater level classes are presented in Figure 6 (Roman symbols). They are characterized in terms of their defined range, and their average level. In the same figure we have plotted the 5 FAO drainage classes, ranging from very poorly drained (VP) to well drained. A comparison between Dutch groundwater maps and FAO drainage classes should validate Figure 6.

3.5 Summary

In order to improve soil routines for meso-scale meteorological models, European soil variability and available methods for its representation have been reviewed. We matched processes already available in more extensive hydrological models and available soil information. The results suggest that scope exists for including additional soil information. The following factors may be added: soil depth, soil salinity, soil texture, soil stoniness and groundwater levels. Soil depth, soil salinity, soil texture and soil stoniness are part of the WISE v 2.1 database. The soil texture data can be used to generate the soil moisture retention curve and the hydraulic conductivity function, using the HYPRES database. The FAO-drainage classification can be used with the soil depth, slope class, and texture information to generate input for a groundwater submodule. A concept has been formulated to translate drainage classes of The Netherlands to the FAO drainage classes. This concept requires further validation.

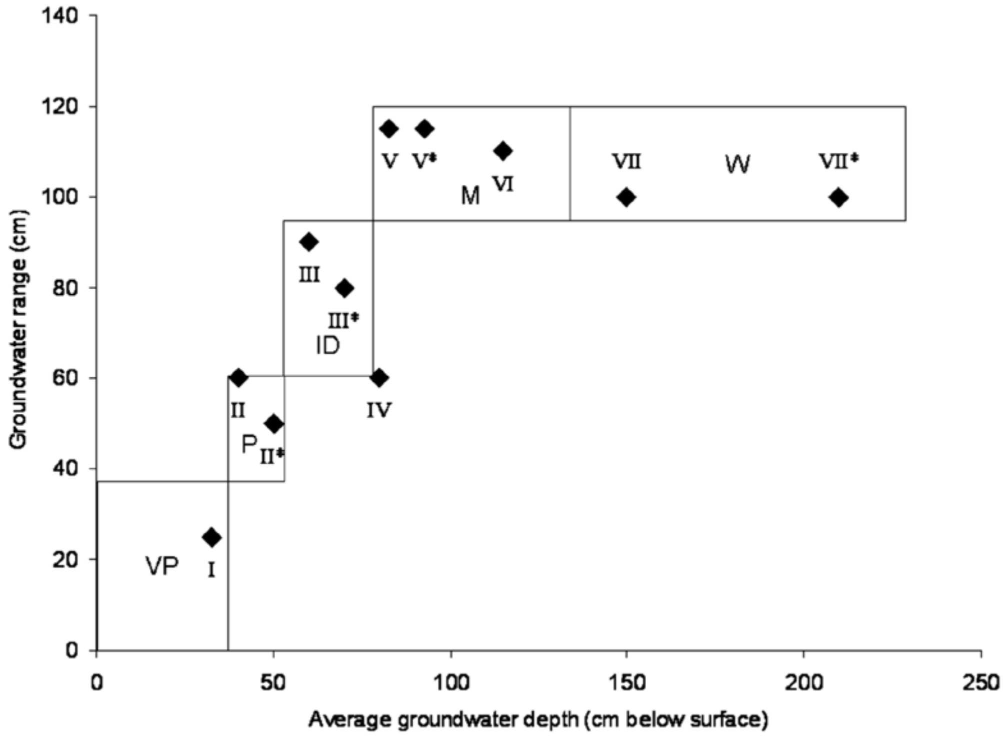

Figure 6.
Translation of drainage classes in The Netherlands (Roman symbols) to the FAO drainage classes (VP - very poorly drained, P: poor, ID: imperfectly; M: moderately well drained, and W: well drained).

4. Root distributions of agricultural crops[3]

4.1 Introduction

Sensible heat, latent heat and the soil ground flux determine the energy balance of the atmosphere near the land surface. In turn, the states of the land surface and the atmosphere determine the partitioning of energy over the three terms of the energy balance. Important land surface state variables are soil moisture and vegetation biomass. Interaction between vegetation and soil determines the amount of evaporated and transpired moisture. The transpired amount is closely related to the biomass production and is at the core of ecological and agricultural analyses of water-limited growth.

Given this strong link to ecosystem productivity, literature on the relations between transpiration, soil moisture and production can be found in agricultural and ecological literature. In agro-

3 Based on Metselaar K., V.L. Versace, R.A. Feddes & J.C. van Dam, 2006c. Root depth distributions. Part 1: Root depth distributions of important agricultural crops. Part 2: Root depth distributions of vegetation types – a reclassification. Reports in the Framework of the KvR project CS3.

hydrological models the description of reduction of transpiration as a function of soil moisture content or soil water pressure head is a key concept. A specific level of evapotranspiration referred to as potential evapotranspiration is a forcing variable in the models, which is partitioned over soil evaporation and vegetation transpiration, using a partitioning function on the basis of soil cover or leaf area index. Subsequently evaporation and transpiration are reduced on the basis of the soil moisture state characterized by either soil moisture content or by soil water pressure head. In models intended for hydrological prediction the process of transpiration reduction is interpreted as a reduction of soil water uptake by the roots. In models intended for meteorological prediction, transpiration reduction is modelled as an increase in stomatal resistance. Functional dependencies between stomatal resistance and various atmospheric state variables have been described by multivariate empirical functions. The paper by Jarvis (1976) is a famous example of this approach. Resistances can be defined at leaf and canopy scale. At present the Penman-Monteith equation is parameterized as a big-leaf equation. For instance canopy data are analyzed as if the canopy effectively behaves as a single leaf.

This issue of scale also arises when analyzing root water uptake. Models for root water uptake have been formulated at the scale of the root system, and at the single root scale. At both scales root density is an important parameter. At the single root scale, root density determines the average distance between roots modelled as parallel tubes. At the scale of the root system an often used hypothesis is to assume that water uptake is proportional to root density (Feddes and Raats, 2004). This Chapter 4 aims to provide inputs for one-dimensional models which evaluate the effects of root systems as actually found in the field (van Noordwijk and van de Geijn, 1996).

Reviews of root density profiles have been presented by O'Toole and Bland (1987) for crops; by Gerwitz and Page (1974) for horticultural species, and by Jackson et al (1996), and Schenk and Jackson (2002) for different biomes. Metselaar et al. (2006c) reviewed the most important agricultural crops. We derived crop root density profiles, following the database setup of Schenk and Jackson (2002), derived the average half mean distance between roots, and assessed the constancy of the parameters over time.

4.2 Methods

Description cumulative root density profiles

The properties of scaled cumulative root density profiles - approaching zero at depth zero and approaching 1 at rooting depth - suggest the use of growth functions. Here we will employ the logistic dose response function as used by Schenk and Jackson (2002):

$$\frac{R}{R_x} = \frac{1}{1+\left(\frac{D}{D_{50}}\right)^c} \qquad (1)$$

with R being cumulative root density, R_x the maximum cumulative root density, D soil depth, D_{50} the depth at which $R / R_x = 0.5$, and c a fitting parameter (> 0).

Introducing the parameter D_{95}, the depth above which 95% of the roots are located, the following relations hold:

$$c = -\frac{\ln(0.95) - \ln(0.05)}{\ln(D_{95}) - \ln(D_{50})} \quad \text{and} \quad D_{95} = \left(\frac{0.95}{0.05}\right)^{-\frac{1}{c}} D_{50} \tag{2}$$

The half mean distance between roots *r* is calculated from the root density *ρ* as:

$$r = \sqrt{\frac{1}{\pi\rho}} \tag{3}$$

It is interesting to analyze under which conditions the cumulative root distribution retains a constant shape over time, as this simplifies modelling assumptions. In case of the logistic dose response function shown above, shape is retained as long as the depth of each cumulative fraction increases with the same relative rate in the entire profile. If this condition is met, the parameter *c* also does not change with time.

Data retrieval

A literature search was performed for the main food crops using Latin names in combination with the term "root length density". Our database setup was similar to Jackson and Schenk (2002). Experimental factors, management parameters (fertilization, plant density and aboveground biomass measurements) were included. In total 53 different sources were analyzed.

Estimates of precipitation and potential evapotranspiration (ET_p) were retrieved from global 0.50 gridded data sets. Precipitation estimates were taken from the 1961-1991 long-term monthly means recorded in the Climate Research Unit (CRU) Global Climatologies. Estimates of ET_p according to Penman-Monteith were retrieved from the data set of Choudhury (1997) and Choudhury and DiGirolamo (1998).

Parameter estimation

The depth-root density data were converted to units of cm and cm cm-3, and numerically integrated over depth to yield the cumulative root length density distribution. Such an integration removes the possibility to estimate parameter confidence intervals as errors are no longer independent. We selected data sets with measurements at more than 4 depths.

We analyzed whether root density functions could be predicted from climatic variables. Therefore non-parametric correlation analyses were carried out between extrapolated D_{50} or extrapolated D_{95} and climatic variables (Spearman rank correlation). The independent climatic variables were Log_{10} (annual precipitation) and Log_{10} (annual evapotranspiration ET_p). The same analysis was done with latitude as the independent variable. Non parametric correlation analysis was used to minimize the effects of unknown errors in the independent variables and extrapolated root depths. The database was analysed as a whole, as monocotyls, and as dicotyls. Further groupings were based upon species and were limited to examples where more than 4 locations were present in the database.

The available data were also used to check whether the parameters describing the root density profile were constant in time. To do so, ordinary least squares linear regression was used. The analysis was restricted to experiments that sampled root profiles more than 4 times during a treatment where experimental conditions remained constant. A total of seven experiments were selected and comprised one with *Helianthus*, four with *Oryza*, one with *Sorghum*, and one with *Triticum*.

4.3 Results and discussion

Model selection and parameter values

A summary of the results for the different growth curves is given in Table 4. The logistic function shows the best calibration results in terms of estimate convergence, goodness of fit, conservative properties at extrapolation, and consistency of analysis in terms of existing databases, notably that of Schenk and Jackson. A good alternative to the logistic function is the Gompertz equation.

Predictive and/or descriptive variables

With the exception of dicotyls, D_{95} correlated with $\text{Log}_{10}\ ET_p$ (n=29, r=0.383, p=0.040), all other combinations were non significant. The apparent lack of correlation between climatic variables, latitude and root density parameters does not contradict results presented by Schenk and Jackson (2002). However, at present, although the database contains 568 root profiles, it contains relatively few locations, and does not allow regional (or climatic) differentiation in parameter values.

Management factors

In contrast to data from natural vegetation, agricultural experiments offer a rich variety of systematically varied factors. However, to quantify the effect of any single factor there should be at least three treatment levels (and preferably more). In combination with the exhaustive root depth sampling required to fit the entire function, it is not surprising that there are few examples at present, where both the complete rooting profile could be fitted, and a quantitative effect of a factor could be established. At present the database contains some examples with 3 nitrogen levels, which show a linear tendency for the parameters to increase with nitrogen level. We have refrained from presenting these results.

Table 4.
Calibration results for 4 selected growth functions.

	Cases with convergence of parameter estimates (n=570)	Cases where D_{95} exceeds maximum measurement depth	R^2_{adj}	Mean D_{50} (cm)	Mean D_{95} (cm)
Generalized logistic	54	5	1.00	32.2	64.4
Logistic	568	48	0.98	26.7	56.0
Exponential	568	422	0.98	46.0	194.2
Gompertz	568	174	0.99	27.2	69.9

Table 5 presents the calibrated parameters describing the average cumulative root density profile for vegetation types defined by Masson et al. (2003). The results are based on a re-analysis of a database published by Schenk and Jackson (2002) and an additional literature review for agricultural crops.

Table 5.
Calibrated parameters describing average cumulative root density profile of different vegetation types.

Vegetation type	n	D_{50}		D_{95}	
		Mean (cm)	SEM[1] (cm)	Mean (cm)	SEM[1] (cm)
Evergreen needle forest	100	18	1	87	4
Evergreen broadleaf forest	90	17	2	99	9
Deciduous broadleaf forest	53	20	2	102	6
C4 herbaceous	16	20	4	120	18
C3 herbaceous	111	11	1	82	5
C4 anthropogenic(tropical pasture)	10	27	7	191	41
C3 anthropogenic (temperate pasture)	18	5	1	49	8
Total agricultural crops	568	27	1	56	2
Wheat (C3)	80	22	1	49	3
Maize (C4)	48	39	3	80	6

(1) Standard Error Mean

Change of root profile shape with time

As in the analysis of management factors, the number of experiments with detailed root profile measurements over time is limited. However, some experiments with rice, sunflower, wheat, and sorghum allowed to test whether the shape parameter c is constant with time. None of the *Oryza* experiments examined for a change in the shape parameter c showed a significant change over the duration of the experiment. In contrast both *Helianthus* and *Triticum* experiments showed a significant decline in c over time. Crop *Sorghum* shows a non-significant result, which may have been influenced by the small number of observations (n=4, Adjusted R^2=0.815, p=0.064). Whereas the degrees of freedom is clearly restricting the analysis, these results are interesting as many models, whilst assuming root depth increases over time, also assume the shape to remain constant. As shown in the theory, this supposes exponential growth for each cumulative root depth class. This issue could very well be addressed with a focused review of literature.

Climate characteristics

At present no significant effects of climate characteristics could be established. This means that at present the database does not support location specific parameter estimates.

Based on the results of the present review, and well aware of its limitations, we find that there is little support for a predictive relationship between parameters of the root density distribution of agricultural crops and climate or management factors. Constancy of the root density distribution parameters with time is shown not to hold in specific cases, but we are far from a predictive relationship. Therefore there is no reason yet to revise or extend root modelling for agricultural crops in climate change models.

4.4 Summary

Root density profiles in soils play a key role in plant transpiration and thus the sensible heat flux. We employed the root data base of Schenk and Jackson (2002) and added recent literature data on root densities of agricultural crops. We tested 4 analytical functions to describe the root data and selected the logistic dose-response function as most suitable function. For this function we calibrated the input parameters for the main vegetation types. These data can be used in both macroscopic and microscopic root water uptake models. We also analyzed whether a correlation exists between root density distribution parameters of agricultural crops and climate or management factors. This correlation was not significant. Constancy of the root density distribution parameters with time is shown not to hold in specific cases, but we are far from a predictive relationship. Therefore at present root density distributions for agricultural crops are described with constant parameters.

5. Evaluation of the land surface scheme HTESSEL[4]

5.1 Introduction

A problem often reported in climate simulations is a systematic summer drying that results in too dry and too warm projections of summertime climate in south-eastern Europe, as shown in Figure 7 (Hageman *et al.*, 2004).

4 Based on Wipfler, E.L, K. Metselaar, J.C. van Dam, R.A. Feddes, E. van Meijgaard, B. van Ulft, B. van den Hurk, S. Swart and W.G.M. Bastiaanssen, 2011. Seasonal evaluation of the ECMWF land surface scheme against remote sensing energy fluxes of the Transdanubian region in Hungary. Submitted to Hydrology and Earth System Sciences.

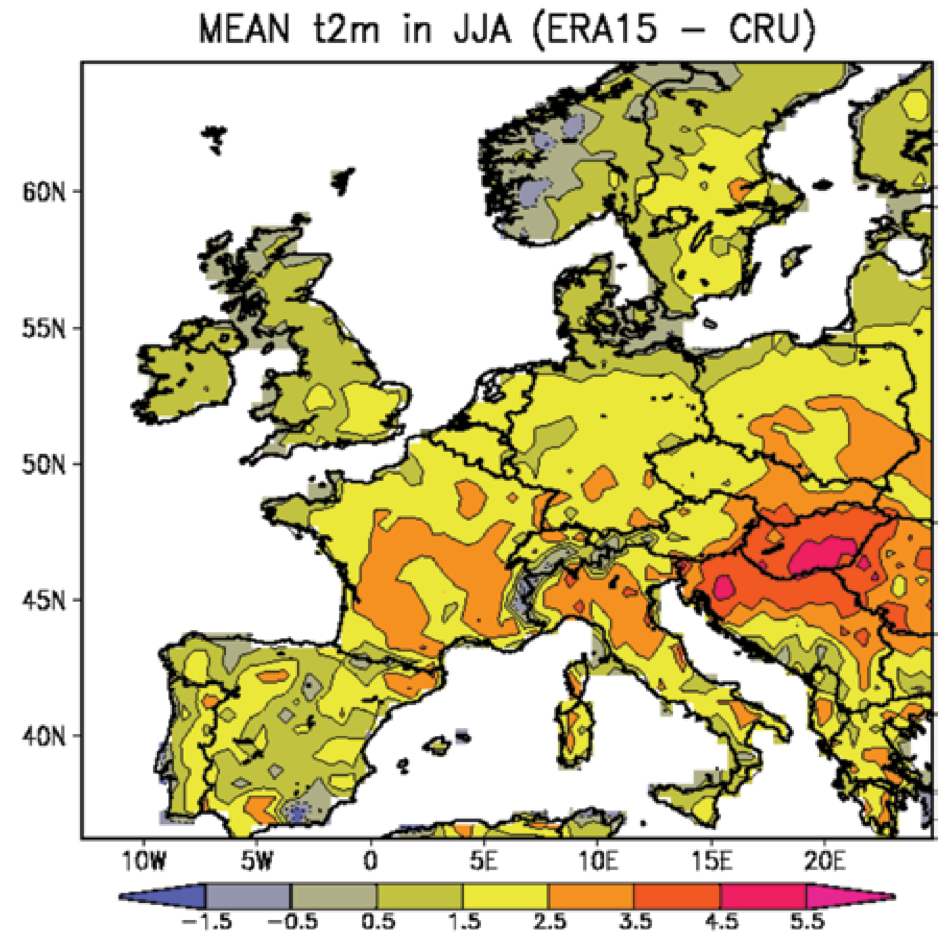

Figure 7. Summer temperature difference between RACMO and ERA15, showing the bias in south-eastern Europe (Lenderink et al., 2003).

This summer drying is associated with a strong reduction of the hydrological cycle, dry soils, strong soil evaporation and plant transpiration stress and reduced precipitation. These models often overemphasize the positive feedback between precipitation and the vapour flux due to soil evaporation and plant transpiration (e.g. Betts *et al.*, 1996, Lenderink *et al.*, 2003; Hageman *et al.*, 2004). Presumably, land surface processes play an important role in this feedback (Fischer *et al.*, 2007a). Improving the representation of the soil hydrological processes may impact the precipitation-evaporation feedback. Using the land surface scheme TESSEL (Tiled ECMWF Scheme for Surface Exchange over Land; Van den Hurk *et al.* (2000)), Lenderink *et al.* (2003) pragmatically solved the tendency of a summer continental dry bias in their Regional Climate Model (RCM) by increasing the soil reservoir depth of TESSEL. It is unclear how realistic this solution is, and whether it is still valid when extrapolating to changing climate conditions.

A new version of TESSEL has been developed (Hydrology-TESSEL; Balsamo *et al.*, 2009) A thorough test with station data and area integrated atmosphere moisture budgets (runoff data, atmospheric water balance data from Hirschi *et al.* (2006) and Seneviratne *et al.* (2004)) confirmed the general improvement of HTESSEL over its predecessor. However, a systematic evaluation of land surface evaporation at a regional scale is deemed necessary to assess the behaviour of a land surface model like HTESSEL in the hydrological feedback cycle. Such an evaluation has been severely hampered by a lack of reliable, spatially explicit surface evaporation data.

This study uses a spatial evaporation estimate for a single growing season (2005) derived from satellite observations to evaluate the spatial variability of seasonal mean surface evaporation from HTESSEL in a central European continental area in the Danube basin. This area appeared particularly prone to pronounced summer drying in the study by Lenderink et al. (2003). The primary objective is to assess the model skill to reproduce spatial gradients of surface evaporation in response to gradients in precipitation and land surface characteristics. A secondary goal is to assess the effect of a number of further model updates.

5.2 The land-surface scheme HTESSEL

In the land surface scheme HTESSEL (ECMWF, 2007; Balsamo *et al.*, 2009) for each grid cell of the atmospheric model the land surface is represented by 6 tiles over land (bare ground, low and high vegetation, intercepted water, shaded and exposed snow). For each tile separately the energy balance is calculated:

$$(1-\alpha_i)R_s^{\downarrow} + R_l^{\downarrow} - R_l^{\uparrow} - G_i = H_i + \lambda E_i \qquad (4)$$

where R_s and R_l (W m^{-2}) are the flux densities of short wave and long wave radiation, respectively, with the arrows refer to incoming (↓) and outgoing (↑) flux densities, α_i is albedo, Hi, λE_i and G_i (W m^{-2}) denote the sensible, latent and soil heat flux density of tile *i*, respectively, λ (J kg^{-1}) the specific latent heat of vaporization and *E* (kg m^{-2}s^{-1}) the mass flux density of evaporation. Total *H*, *G* and λE are calculated as the area weighted average over the tiles. Soil heat is redistributed over a fixed vertical grid of 4 soil layers (extending to 2.89 m depth) using a standard diffusion scheme, allowing for thermal contributions from soil water freezing and melting (Viterbo *et al.*, 1999).

Turbulent heat and water vapour fluxes from each tile are calculated using a resistance analogy, where an aerodynamic and surface resistance accounts for the transfer efficiency of heat or water vapour over a vertical temperature and humidity gradient. The surface resistance r_c is a function of $R_s^{\downarrow}$, leaf area index *LAI* (m^2 m^{-2}), average unfrozen soil water content θ (m^3 m^{-3}), atmospheric water deficit D_a (Pa), and minimum stomatal resistance $r_{s,min}$ (s m^{-1}) (Jarvis, 1976):

$$r_c = \frac{r_{s,min}}{LAI} f_1(R_s^{\downarrow}) f_2(\bar{\theta}) f_3(D_a) \qquad (5)$$

In particular, the sensitivity of evaporation to soil water content is relevant to discuss here, as it affects the seasonal evolution of evaporation and soil water content, i.e.:

$$f_2^{-1} = \frac{\bar{\theta} - \theta_{wp}}{\theta_{fc} - \theta_{wp}} \qquad (6)$$

where θ_{wp} and θ_{fc} are the soil water contents at permanent wilting point and at field capacity, respectively, and $\overline{\theta}$ is the root density weighted average water content over all soil layers of the unfrozen soil water. Hence, when $\overline{\theta} < \theta_{fc}$ the resistance increases and becomes infinite at wilting point. Vertical root density distributions have been derived following Zeng *et al.* (1998) and adapted to a multilayer configuration. Coefficients for f_1, f_2 and f_3 are taken from a lookup table, for which an externally prescribed vegetation type forms the entry. Vegetation data are derived from ECOCLIMAP (Masson *et al.*, 2003).

The water balance (mm d -1) at the land surface is described by:

$$\Delta W + \Delta S = P - E - R \qquad (7)$$

where ΔW represents the change in water storage of the soil moisture and interception reservoir, ΔS the change in accumulated snowpack, P represents precipitation, E represents evaporation of soil, vegetation and intercepted water, R surface and subsurface runoff.

Initially, precipitation is collected in the interception reservoir until it is saturated. Then, excess precipitation is partitioned between surface runoff and infiltration into the soil column. When the imposed water flux exceeds the maximum possible soil infiltration rate, excess water is taken as surface runoff as described by the so-called Arno scheme, while accounting for sub-grid variability related to orography (Dümenil and Todini, 1992; Van den Hurk *et al.*, 2002).

Soil water flow in HTESSEL is described by the diffusivity form of the Richards' equation using the same four-layer discretization as for soil temperature (with increasing thickness from the soil surface downwards, i.e. 0.07 m, 0.21 m, 0.72 m and 1.89 m). The dependencies of the soil hydraulic conductivity k ($m\ s^{-1}$) and soil water diffusivity D ($m^2\ s^{-1}$) on θ are described by means of the analytical functions of Van Genuchten (1980). Hydraulic coefficients are specific for 6 soil textures, i.e. coarse, medium, medium-fine, fine, very fine and organic.

HTESSEL does not account for either lateral exchange of soil water between the grid elements and/ or irrigation. Excess water leaves the domain as either surface or subsurface runoff. At the bottom of the soil column, free drainage is assumed. Alternative lower boundary conditions are not considered.

5.3 Site and observations

5.3.1 Transdanubian test region

The test region covers the Western region of Hungary between approx. 45.5 - 48.5°N and 16.0 - 20.0°E being the Transdanubian region. Most of the area is flat and bounded by the Alps in the Southwest and the Tatra in the Northwest. The climate of Hungary can be described as a typical European continental climate with warm, dry summers and fairly cold winters. Average precipitation, P is 612 mm yr^{-1} and the average annual temperature at 2 m height, T_{a2m} is about 10 °C. The average summer T_{a2m} is approximately 19.6 °C and the average winter T_{a2m} is 0.4 °C (Szalia *et al.*, 2005). The soils in the area can be classified as acid and non-acid loamy, well-drained soils, salt affected, sodium rich and imperfectly drained soils (Dobris report, Soil map of Europe, 1995). About 2/3 of the land is under cultivation. The remaining vegetation is mainly deciduous forest and mixed forest (Masson *et al.*, 2003). In Figure 8 the percentage of areas under irrigation is given for the area considered (Siebert *et al.*, 2007), which reveals that along the Danube valley the percentage of irrigated land is up to 50%. The annual amount of irrigated water associated with these figures is unknown, e.g. it depends on the type of crop, irrigation technique, climate and season.

Measurements taken at the two flux-towers from the CarboEuropeIP database (Tuba *et al.*, 2005) being located in Matra and Bugac (see Figure 8), were used as ground truth of the satellite observations. Both towers are situated in a grassland ecosystem.

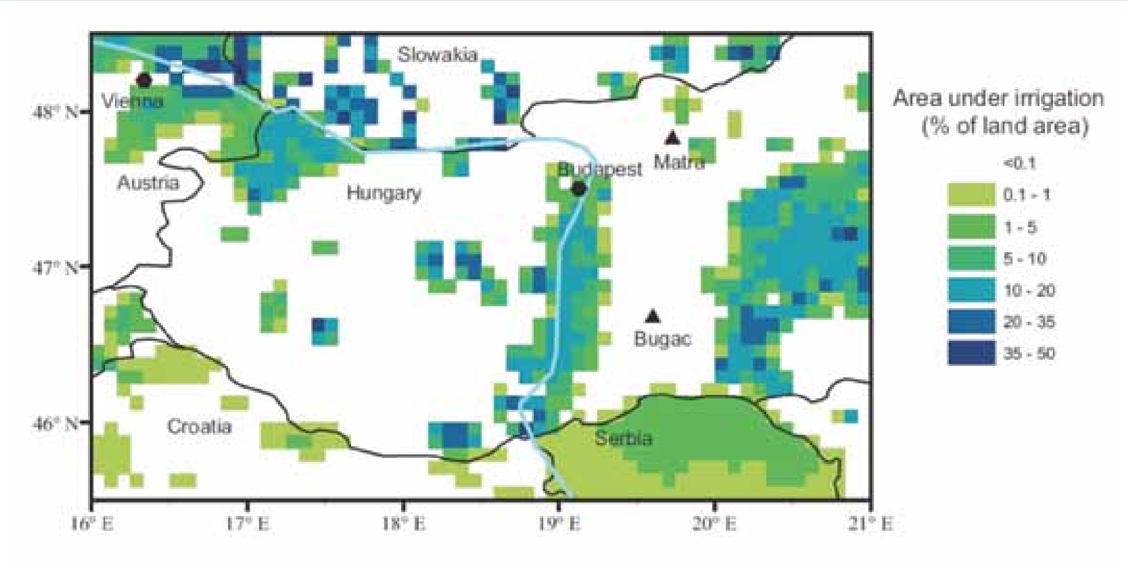

Figure 8.
Transdanubian test region and percentage of irrigated area obtained from the global map of irrigation areas provided by the FAO's global information system on water and agriculture at a resolution of 5′ (Siebert *et al.*, 2007). The black lines represent country boundaries. The light blue line indicates the river Danube. The locations of the meteorological towers Matra and Bugac are indicated with black triangles.

5.3.2 Areal precipitation using TRMM

Area covering space-born precipitation, *P*, is provided by the Tropical Rainfall Measuring Mission (TRMM) on a monthly basis at a resolution of 0.25°. Comparison of the space-born annual precipitation with the precipitation measured at 35 weather stations in the region shows that in 2005 TRMM appears to over-predict precipitation. This occurs especially in low precipitation areas, where differences could be up to 400 mm. Therefore, we corrected the TRMM precipitation using the linear regression relation between satellite and ground observations on an annual basis (see Figure 9-top). The corrected annual TRMM precipitation over the test area is given in Figure 9-bottom. The standard deviation of the corrected annual TRMM precipitation as compared to the meteostation data was 85.2 mm. Annual precipitation over 2005 was on average 652 mm. The highest annual precipitation (around 900 mm) was measured in the mountainous south-western and north-eastern part of the region. In the Danube valley including Lake Balaton, the annual precipitation was low, down to 450 mm.

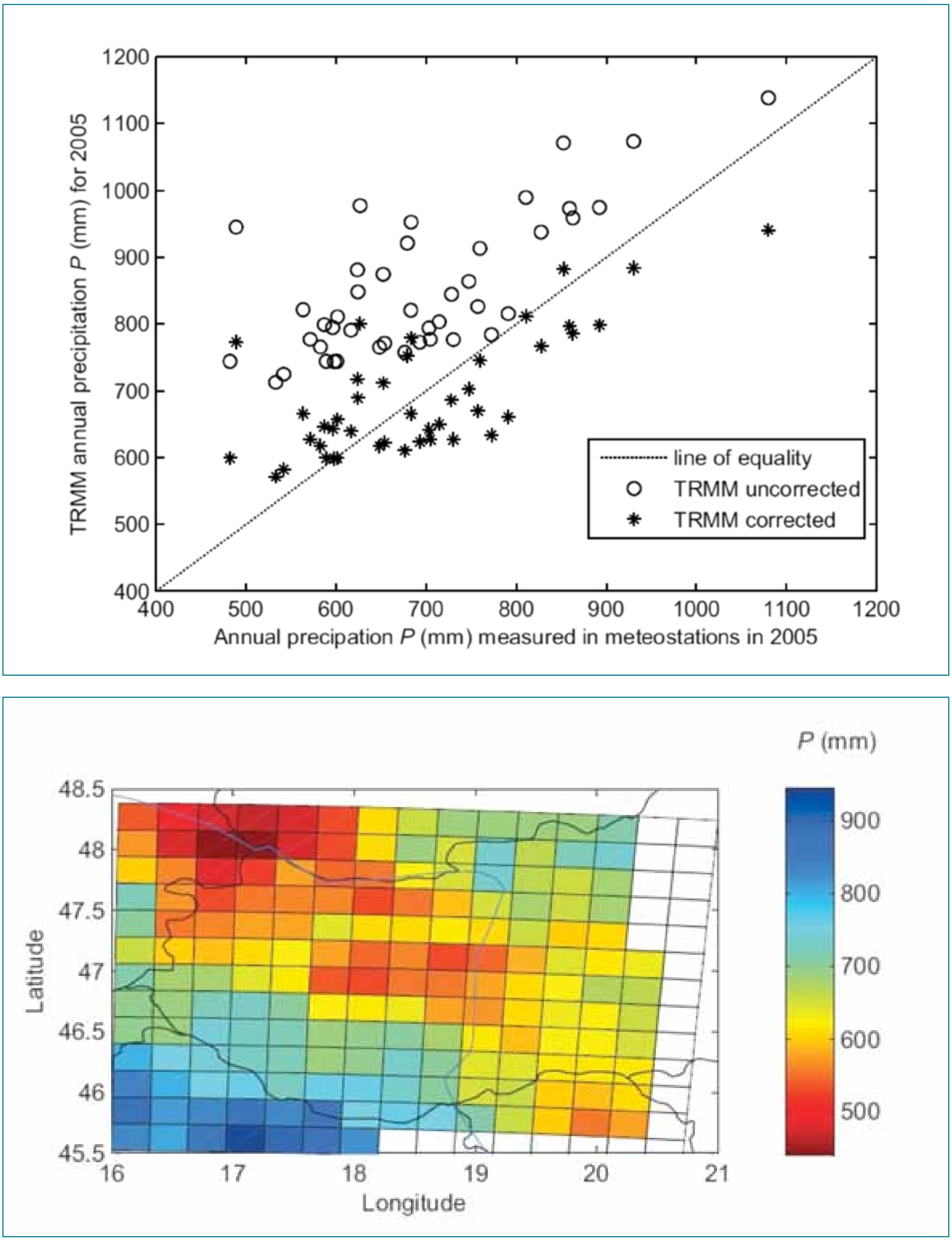

Figure 9.
Annual precipitation *P* (mm) over 2005 in the test area (top) measured at meteostations and the corresponding corrected and uncorrected TRMM observations and (bottom) corrected TRMM observations, being projected at a spatial resolution of 0.25 °.

5.3.3 Energy fluxes from satellite images

SEBAL algorithm

The Surface Energy Balance Algorithms for Land Maps (SEBAL, Bastiaanssen *et al.* 1998) was applied to obtain high-resolution maps of the actual evapotranspiration. SEBAL is an energy partitioning algorithm that solves the energy balance at the surface pixel wise from satellite images and standard meteorological measurements. Standard inputs are satellite derived maps of the Normalised Difference Vegetation Index (NDVI), surface albedo and surface temperature and measurements of the air temperature, wind speed, relative humidity and incoming short wave radiation obtained from meteorological stations.

Updates of the algorithm's first version, as outlined in Bastiaanssen *et al.* (1998), are provided by Bastiaanssen (2000) and Bastiaanssen *et al.* (2005). SEBAL has ever since its development been tested and validated over a wide range of surfaces under varying climatic conditions. These included natural vegetation and agricultural crops under water-stressed as well as well-watered conditions. A summary of these validations studies, the methods of validation, and the accuracies that were found, are provided in Bastiaanssen *et al.* (2005). They found that on a daily basis the accuracy of the ET_{act} estimation is around 15% whereas for seasonal or annual ET_{act} estimations an accuracy of approximately 5% may be reached. A full explanation of SEBAL goes beyond the scope of this Chapter and reference is made to the previously cited work by Bastiaanssen. Some basic background is provided in the section below.

The latent heat fluxes are computed following Eq. (4). Daily net radiation R_{n24} (W m^{-2}) is computed in SEBAL using satellite measured broadband surface albedo α, extraterrestrial solar radiation $R_{s,exo}^{\downarrow}$ (W m^{-2}) and incoming short wave radiation (ground truth) $R_s^{\downarrow}$ according to De Bruin and Stricker (2000):

$$R_{n24} = (1-\alpha)R_s^{\downarrow} - 110\frac{R_s^{\downarrow}}{R_{s,exo}^{\downarrow}} \qquad (8)$$

The soil heat flux density G (W m^{-2}) is computed as a variable fraction of R_n, taking into account the presence of leaves by means of the Normalized Difference Vegetation Index (NDVI) and the surface temperature (warmer surfaces have higher G/R_n fractions). The sensible heat flux density H is estimated following the standard Monin-Obukhov theorem for turbulent exchange processes and thermal convection. For this pixel wise forcing, air temperature, relative humidity and wind speed are required. Prior to the single pixel computation, extreme values of H are determined. An extreme wet pixel is identified based on the map of the surface temperature and the NDVI, and for these conditions it is assumed that $H = 0$. Similarly, an extremely dry pixel is selected where H is set equal to $R_n - G$.

In order to infer weekly estimates of the surface energy fluxes in the year 2005, the SEBAL algorithm was applied for 19 cloud-free images of the test region from the Terra and Aqua sensors onboard of the MOderate Resolution Imaging Spectrometer (MODIS) satellite. This satellite passes daily and the thermal bands, which are dominant in the SEBAL calculations, have a spatial resolution of 1 km. Meteorological data were obtained from 35 stations in Western Hungary and bordering countries and spatially interpolated to 1 km grids by using an interpolation method that includes land use, vegetation density and elevation (Voogt, 2006). Since $R_s^{\downarrow}$ was not available from the 35 meteorological stations, $R_s^{\downarrow}$ from the Bugac and Matra flux-towers was used instead. The measurements from the two towers have been averaged and used as input to the SEBAL calculations, hence ignoring spatial patterns of incoming radiation. The weekly energy fluxes were obtained by re-applying the SEBAL algorithm with the average meteorological data for the week considered. The bio-physical parameters such as surface albedo, NDVI, emissivity, surface roughness and bulk surface resistance, were estimated at the time of cloud free satellite observations and assumed constant over the cloudy period. This method has been tested and validated over a wheat dominated area in Mexico (see Zwart and Bastiaanssen, 2007).

SEBAL evaporation in the Transdanubian region

In Figure 10 the SEBAL seasonally averaged evaporative fraction $\lambda E / R_n$ is given. Data are downscaled to the model spatial resolution of 0.25°. The considered growing season covers 30 weeks and starts at week 13 (March 26th 2005). The spatial pattern of $\lambda E / R_n$ is similar to the spatial pattern of precipitation shown in Figure 9, which suggests that $\lambda E / R_n$ is to a large extent controlled by precipitation. Fig. 11 shows the relationship between annual P (mm, TRMM product) and seasonal E (mm) for each grid cell. For low P ($450 < P < 750$ mm), E monotonically increases with P, suggesting moisture-limited evaporation. For larger P (> 750 mm) evaporation ceases to increase, pointing to radiation-controlled evaporation. The grid cells situated above the 45°-line $E = P$ may need additional recharge to sustain the evaporation rates ($P - E$) < 0. This phenomenon can also be observed in Figure 12, which shows a map of the water balance deficit (potential recharge), i.e. the difference between TRMM P and SEBAL E. The red grid cells ($P - E < 0$) are situated along the river Danube, which is known to contain irrigated cropland (see Figure 8), and could be influenced by shallow groundwater that facilitates capillary rise of water inside the soil column. These areas coincide with low precipitation areas. The blue areas, where $P - E > 200$ mm, are mainly characterized by mountainous terrain related to lateral (sub) surface flow as well as lower soil thickness (and therefore reduced water availability and lower E).

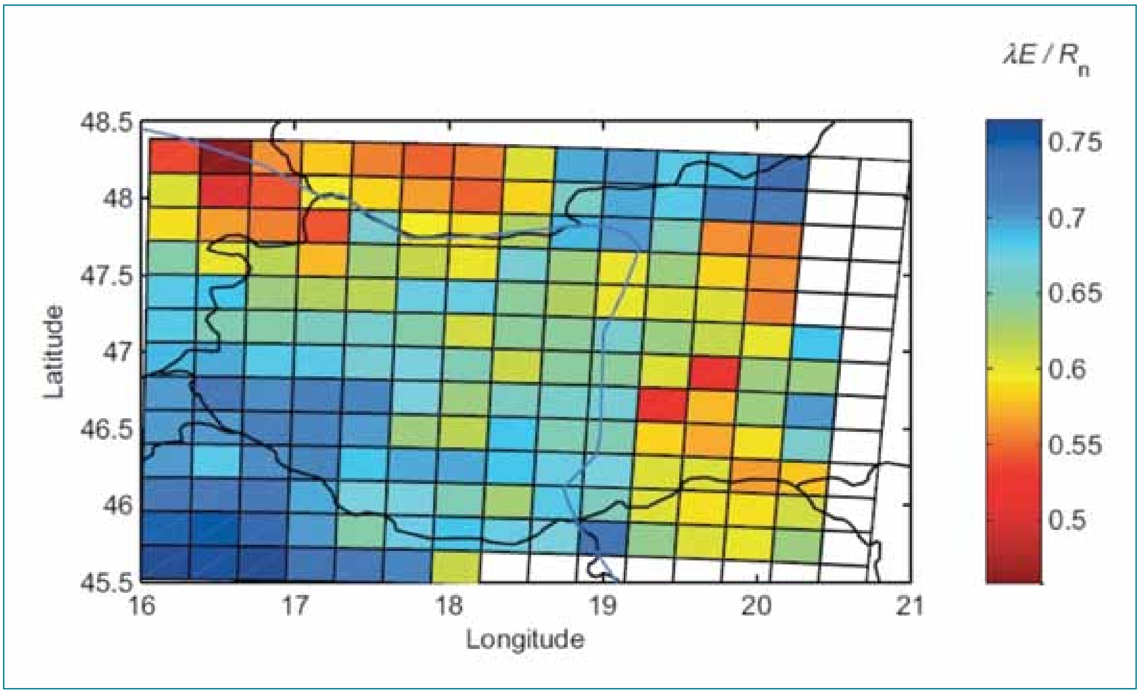

Figure 10.
Map of seasonally averaged daily $\lambda E / R_n$ for the Transdanubian test region in 2005. $\lambda E / R_n$ has been derived from satellite images using SEBAL. The spatial resolution is 0.25 °.

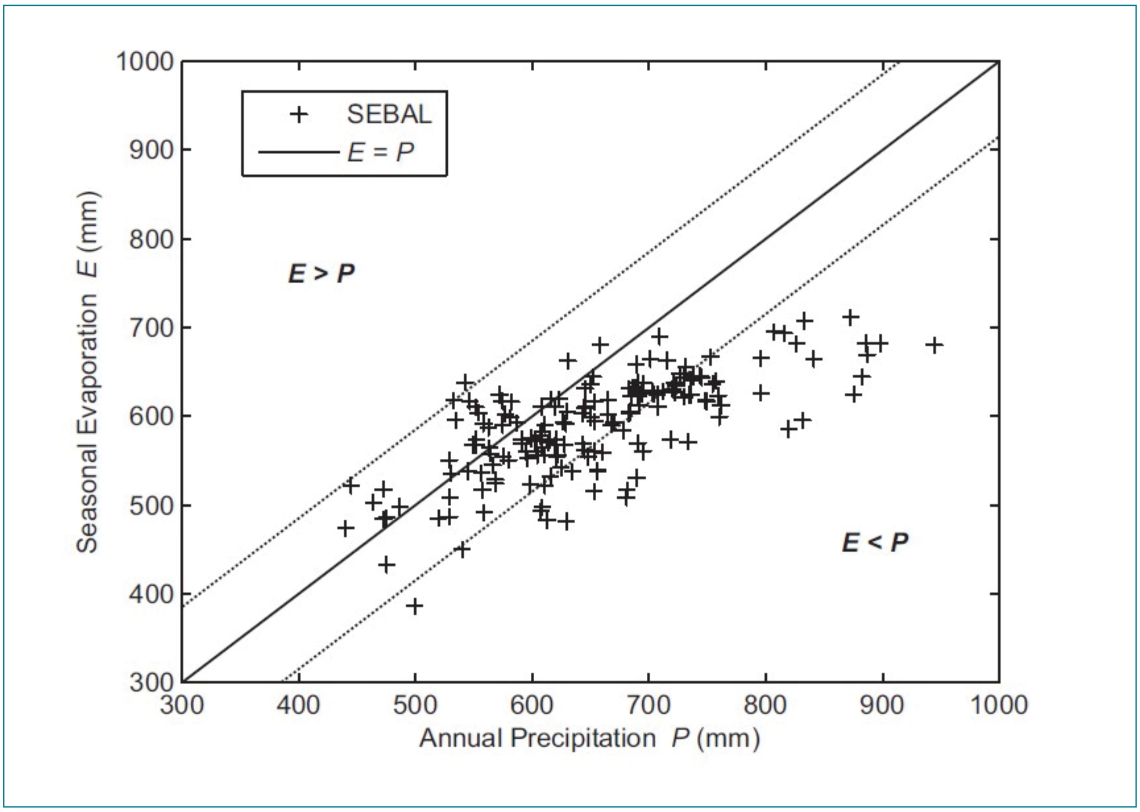

Figure 11.

Seasonal SEBAL derived evaporation *E* (mm) over a 30 week period in 2005 starting at week 13 and ending at week 43 and annual TRMM precipitation *P* (mm) over 2005 for each grid cell in the test region. Each point represents a grid cell. The line *E* = *P* is given for reference as well as the dotted lines representing *E* = *P* ± the standard error of TRMM *P*.

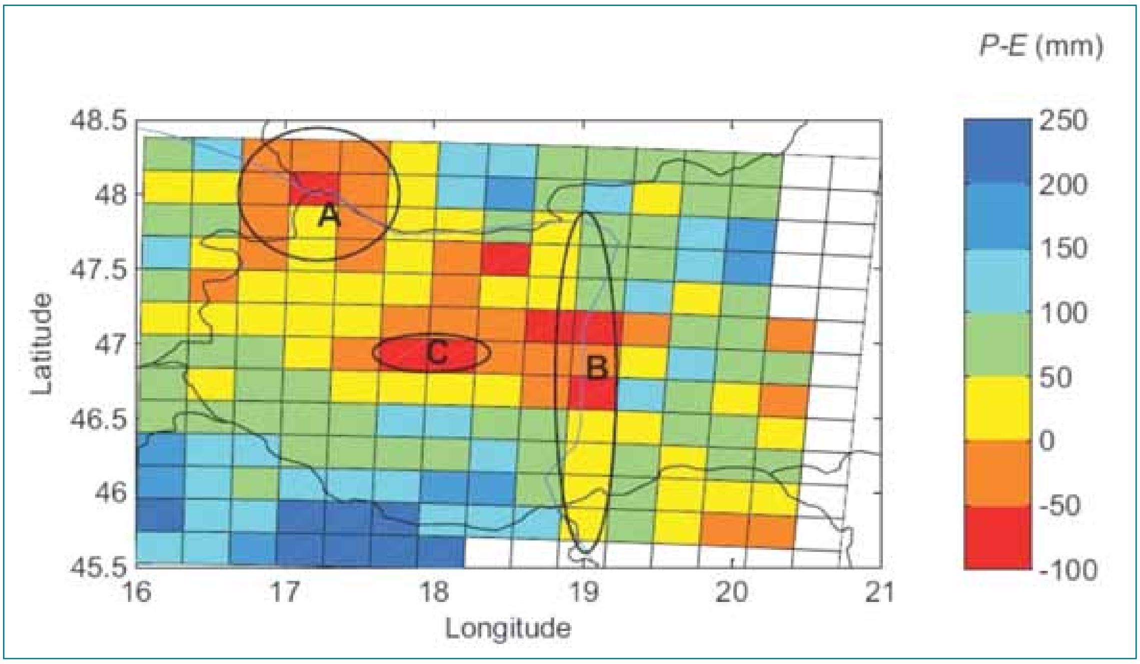

Figure 12.

Potential recharge (Annual P_{TRMM} – Seasonal E_{SEBAL}) over 2005 in the Transdanubian region. The areas A and B represent irrigated cropland area and C represents lake Balaton.

5.4 HTESSEL model setup and input data

5.4.1 Atmospheric forcing

The test domain has been divided into 170 grid cells at a resolution of 0.25°. For this domain, simulations covering the entire year 2005 have been executed. HTESSEL was forced using 3-hourly fields of precipitation *P*, radiation $R_s\downarrow$ and $R_s\downarrow$, temperature T_{a2m}, humidity *q* and wind speed at 10 m height *u*. These fields were derived from a simulation with the Regional Atmospheric Climate Model (RACMO2.1; Van Meijgaard *et al.*, 2008) driven by ECMWF operational analysis. This set-up was preferred above interpolation of ERA-40 data, to avoid imbalances in the atmospheric driving fields originating from the data assimilation applied in ERA-40 (Uppala *et al.*, 2005). With this set-up the right synoptic variability has been retained as well as atmospheric forcing variables that were in mutual agreement.

5.4.2 Soil and vegetation data input of HTESSEL

Soil hydrologic parameters were taken from the FAO soil map and database at a spatial resolution of 5' (FAO, 1995). Soil textural information of the FAO soil types has been translated to six texture classes: coarse, medium, medium-fine, fine, very fine and organic. For each of the soil texture classes the hydraulic conductivity and the Van Genuchten coefficients were specified (see also Van den Hurk en Viterbo, 2003). The dominant soil type was used for each grid cell. Vegetation parameters were provided by the ECOCLIMAP vegetation map (Masson *et al.*, 2003) at a resolution of 5' and translated to high and low vegetation tiles.

5.4.3 Initial conditions of HTESSEL soil state variables

Initial water in the soil system serves as a water reservoir that is available for evaporation in times of low precipitation. The proper estimation of initial soil water and snow may have significant effect on the accuracy of the model. To show this HTESSEL has been run for two sets of initial conditions. These sets contain soil moisture, intercepted water, snow water mass, snow temperature, snow density and soil temperature. Set 1 consists of initial conditions from the hind cast run of RACMO driven by ECMWF operational analysis. Set 2 uses an equilibrium initial state, obtained by cycling the model through the 2005 forcing until equilibrium was reached, i.e. using the convergence criterion of less that 1.25% difference in total soil water volume. In Table 6 mean, maximum and minimum of the initial total soil water storage (mm) and the water equivalent snow thickness (mm) in the grid cells are given for Set 1 and 2. Soil water storage differs greatly between the two sets, implying a large difference in the total annual amount of water that is available for evaporation. Set 2 has considerable higher initial soil water variability and a thicker overall snow pack than Set 1. The relatively large snow layer for Set 2 is caused by the heavy snowfall at the end of 2005.

Table 6.

Mean, maximum and minimum model grid values of initial soil water storage and initial water equivalent snow. Set 1 is the initial condition set that originates from the RACMO hind cast run, Set 2 is the equilibrium initial state condition.

	Soil water storage (mm)		Water equivalent snow (mm)	
	Set 1	Set 2	Set 1	Set 2
Mean	782	732	0.2	20
Minimum	625	241	0	1
Maximum	967	1150	2	51

5.5 Results of HTESSEL calculations

The HTESSEL model skills to reproduce surface evaporation were evaluated by comparing the HTESSEL evaporative fraction $\lambda E / R_n$ with SEBAL derived $\lambda E / R_n$ for initial condition Sets 1 and 2. The evaporative fractions are averaged over the growing season, starting the 26th of March 2005 and ending 30 weeks later in the same year.

In Table 7 the mean, variance and the 10th and 90th percentile of the seasonally averaged $\lambda E / R_n$ are given for SEBAL and HTESSEL Sets 1 and 2. The HTESSEL mean and 90th percentile values of $\lambda E / R_n$ correspond very well to SEBAL. The 10th percentile of HTESSEL is lower than SEBAL, which indicates a small offset towards lower $\lambda E / R_n$. The RMSE's of the model simulations are approximately 9% of the mean SEBAL $\lambda E / R_n$. This is larger than the accuracy of SEBAL, which is on a seasonal basis approximately 5%.

Table 7.
Mean, 10th and 90th percentile of $\lambda E / R_n$ from SEBAL and HTESSEL for the initial conditions 1 and 2. The RMSE of the HTESSEL model predictions is given in the last row.

	SEBAL	HTESSEL	
		Set 1	Set 2
Mean $\lambda E / R_n$	0.64	0.62	0.62
10th percentile $\lambda E / R_n$	0.56	0.53	0.54
90th percentile $\lambda E / R_n$	0.71	0.70	0.71
RMSE $\lambda E / R_n$	-	0.06	0.055

In Figure 13 the difference between SEBAL and HTESSEL seasonally averaged $\lambda E / R_n$ is given as percentage of SEBAL $\lambda E / R_n$ for Set 1 and 2, respectively, for each grid cell. The maximum prediction error is 30 %. The figures reveal that initial conditions have a considerable impact on the spatial distribution of calculated $\lambda E / R_n$.

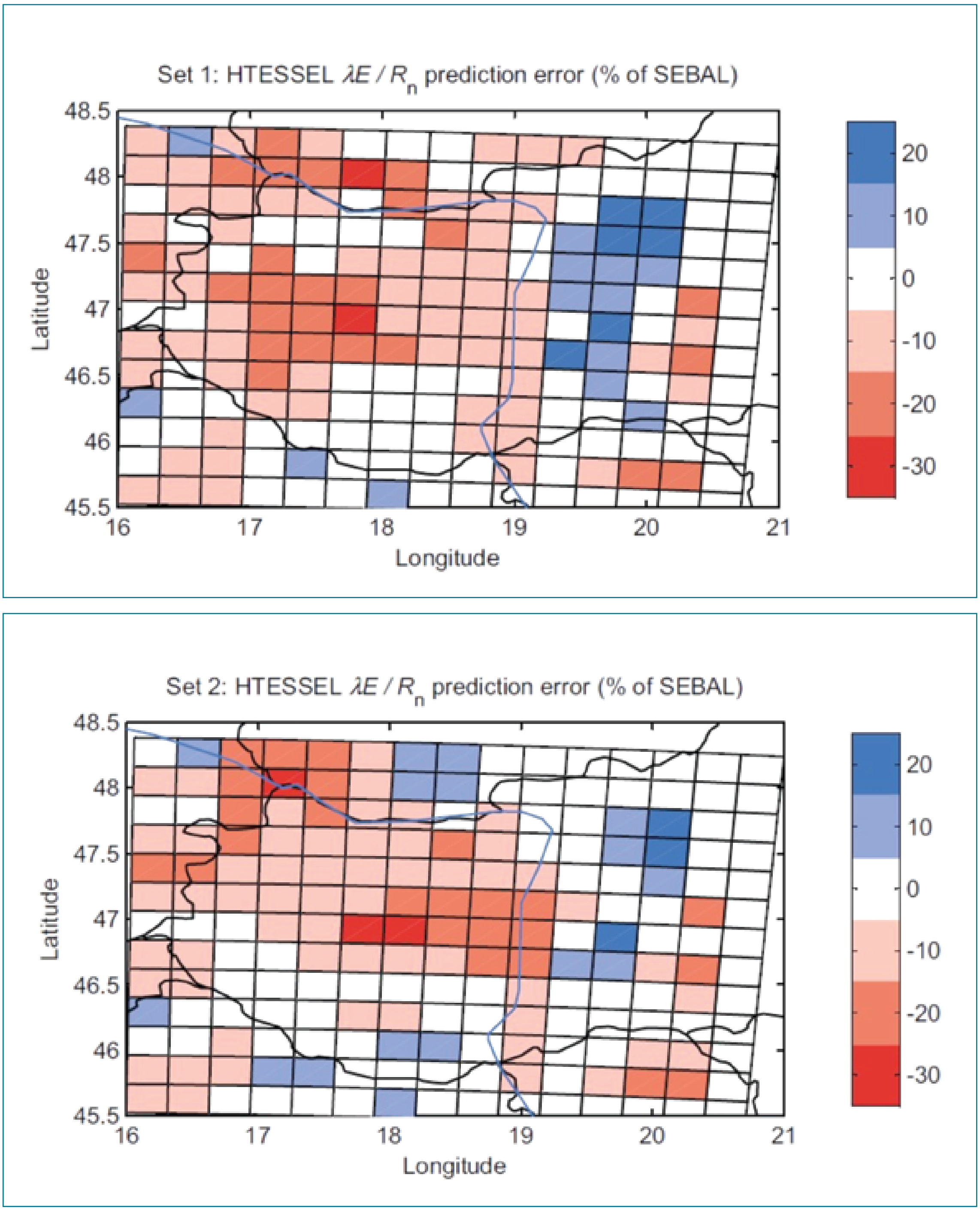

Figure 13.
Difference between SEBAL and HTESSEL seasonally averaged evaporative fraction, $\lambda E / R_n$ as percentage of SEBAL $\lambda E / R_n$ for initial condition Set 1 and 2, respectively. The blue cells refer to $\lambda E / R_n$ over prediction, the red cells to under prediction by the model.

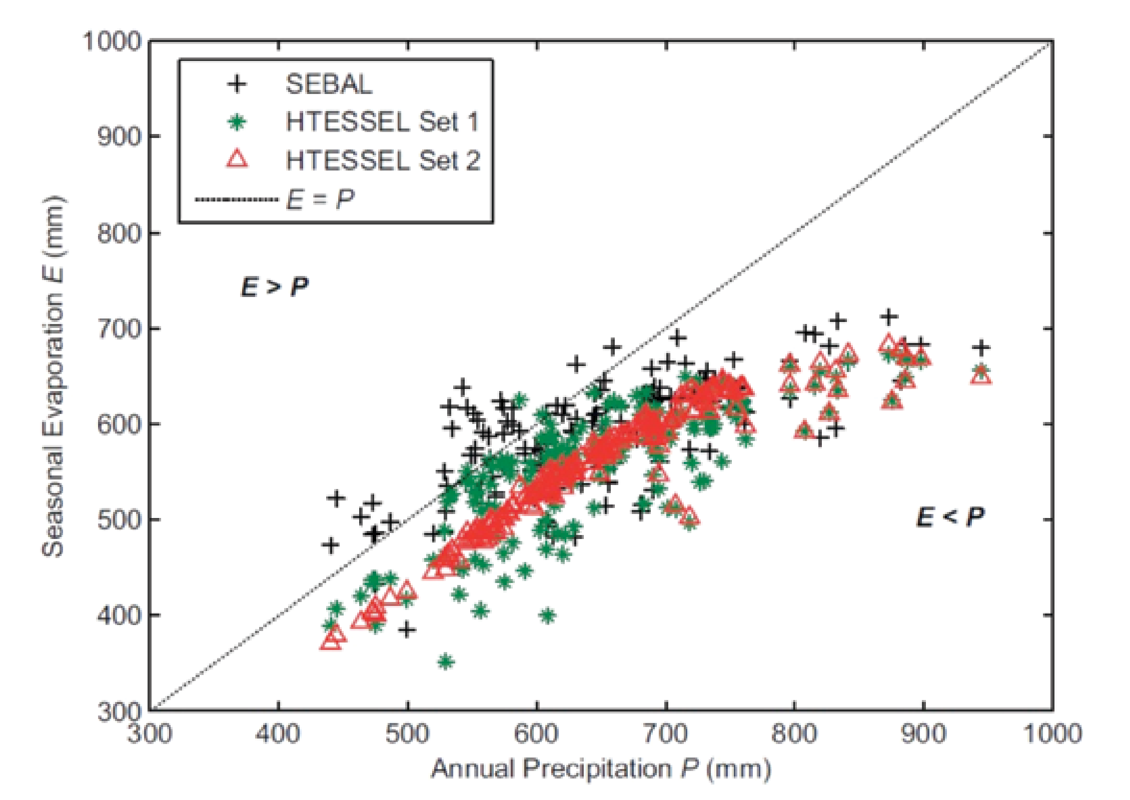

Figure 14.
Seasonal SEBAL and HTESSEL derived *E* (mm) over a 30 week period starting at week 13 and ending at week 43, 2005 and annual TRMM precipitation (*P*, mm) over 2005 for each grid cell in the test region. Each point represents one grid cell. The dotted line *E* = *P* and SEBAL *E* are given for reference. Like Figure 11, the figure shows a correlation between *P* and *E*, especially for Set 2. For both initial condition sets the transition between precipitation dominated *E* and radiation dominated *E* is clearly visible.

In Figure 14 calculated seasonal evaporation is plotted against yearly TRMM precipitation for SEBAL and the two model calculations. Similar to SEBAL $\lambda E / R_n$, the calculated $\lambda E / R_n$ is precipitation dominated, especially for initial condition Set 2. The figure further reveals that HTESSEL's skill to reproduce evaporation in areas with negative potential recharge appear to be poor for both initial condition sets.

5.6 Design and evaluation of modifications to HTESSEL

As discussed in Chapter 2, Metselaar *et al.* (2006a) analyzed the sensitivity of calculated turbulent surface fluxes to 15 different soil process parameterizations for two climates: Continental and Atlantic. The detailed and flexible soil-water-atmosphere model SWAP that is generally used for agrohydrological studies (Kroes *et al.*, 2008), has been employed for this analysis. The analysis indicates that especially the treatment of the lower boundary condition (free drainage, irrigation, capillary rise from groundwater) and rooting depth, but also the depth of the soil column, may have a significant effect on the partitioning of radiant energy over latent, sensible and soil heat fluxes. Additionally, Metselaar *et al.* (2006a) showed that transpiration timing strongly responds to a change of the evaporation reduction function, i.e. from a function of volumetric soil moisture to a function of soil water pressure head. Besides, Metselaar *et al.* (2006a) indicated that a finer mesh of the soil column yields improved convergence. Given these results, we incorporated and evaluated a number of modifications to HTESSEL that are discussed below.

5.6.1 The effect of water stress on the canopy resistance

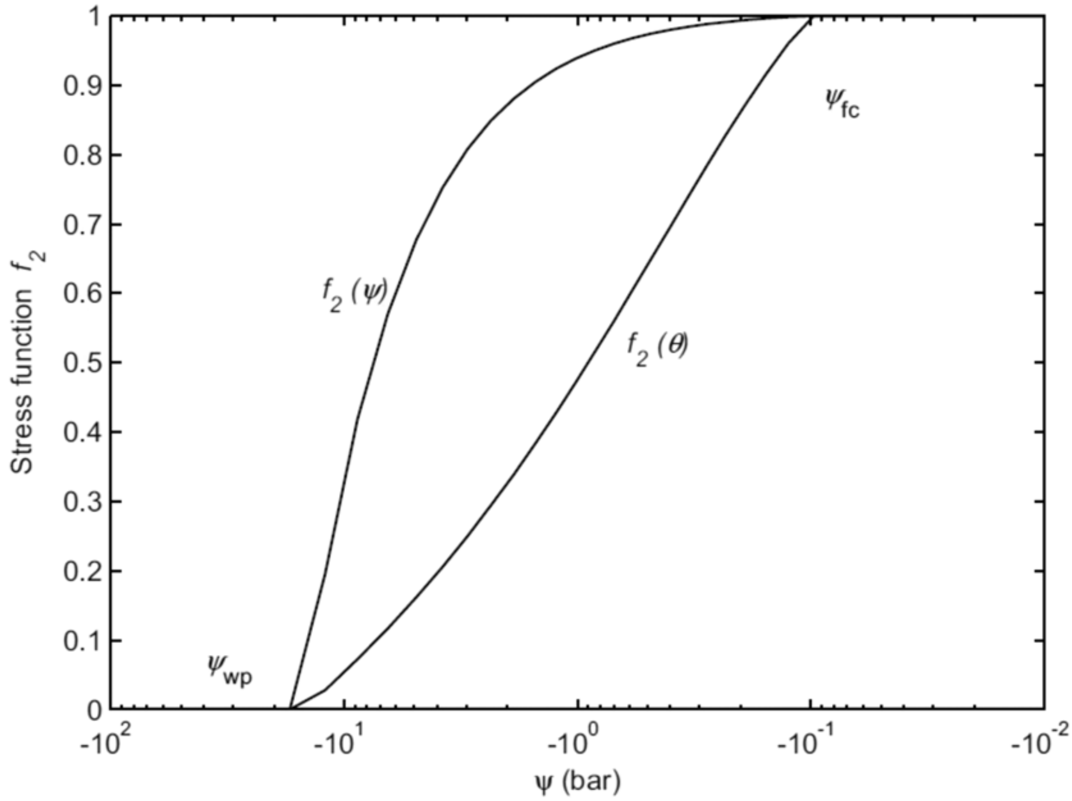

Figure 15.
The functions f_2 (θ) and f_2 (ψ) as related to soil matric pressure. The hydraulic properties of the soil are: k = 0.26 e^{-6} (m s^{-1}), n = 1.25, α = 0.83 m^{-1}, θ_{max} = 0.43 and θ_r = 0.01. The functions f_2 (θ) and f_2 (ψ) have been calculated according to Eqs. (6) and (9), respectively.

We changed the function f_2 in Eq. (6) to a (more physically based) water pressure dependent expression as:

$$f_2^{-1} = \frac{\psi(\bar{\theta}) - \psi_{wp}}{\psi_{fc} - \psi_{wp}} \qquad (9)$$

where ψ (bar) is the soil matric pressure, defined as the air pressure minus the water pressure. The matric pressure of the permanent wilting point (ψ_{wp}) and the field capacity (ψ_{fc}) is -15 bar and -0.1 bar, respectively. For $\psi < \psi_{fc}$, f_2 decreases from 1 at field capacity to 0 at wilting point. In Figure 15, the functions f2 as defined by Eq. (6) and Eq. (9), respectively, have been depicted as a function of ψ. Especially in the frequently occurring ψ range between -10 and -0.2 bar the difference in reduction is large.

5.6.2 Soil depth classes

To replacing the fixed soil column depth of 2.89 m, spatially variable soil depths were constructed based on the Digital Soil Map of the World and Derived Soil Properties version 3.5 (FAO, 1995). Given the soil type at the FAO soil map and the soil name, phase and drainage class, taxotransfer rules were used to determine the soil depth classes at the spatial resolution of the FAO map (5'). These rules have been developed by Van Dam *et al.* (1994) in the framework of a European Crop Growth

Monitoring System. We distinguished between five soil depth classes: soil depths of 10 cm, 60 cm, 80 cm, 100 cm and > 100 cm (i.e. 2.89 m). A map of soil depths in the test region is given in Figure 16. 30% of the test region has a soil depth that is shallower than 2.89 m. For this part of the region, the original model input soil depth has to be changed to more physically realistic depths.

5.6.3 Shallow groundwater

As no upward flow from groundwater is possible in the current HTESSEL model, this effect is represented by introducing extra storage for soils with shallow groundwater. For this the van Genuchten retention parameter α was changed such that the effective soil moisture at field capacity increased by 10%. To obtain a global map of soils influenced by shallow groundwater, the method proposed by Van Dam *et al.* (1994) was applied to FAO soil type data, i.e. Gleysoils, Phaeozems, Fluvisols, Histosols, Gleyic Podsols were labelled as being groundwater affected. Figure 16 shows the affected grid cells in the test region.

5.6.4. Evaluation of the HTESSEL modifications

Four cases have been evaluated, and compared to the reference HTESSEL. In Case 1 f_2 was revised. In Case 2 a variable soil depth was applied. Case 3 considers the effect of shallow groundwater. Case 4 combines Cases 1, 2 and 3. Additionally, we doubled the number of soil layer from 4 to 8 for all Cases. Since, the number of soil layers did not affect the calculated $\lambda E / R_n$, this modification is not discussed separately as a case. We used two sets of initial conditions (see Table 6). The evaluated cases are listed in Table 8.

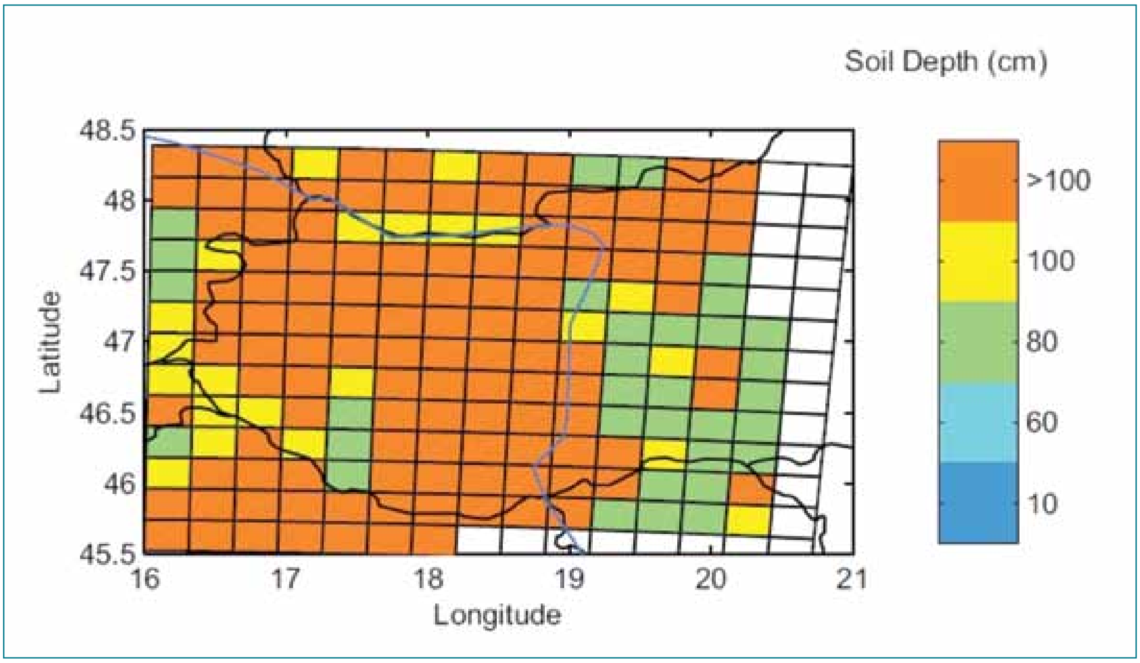

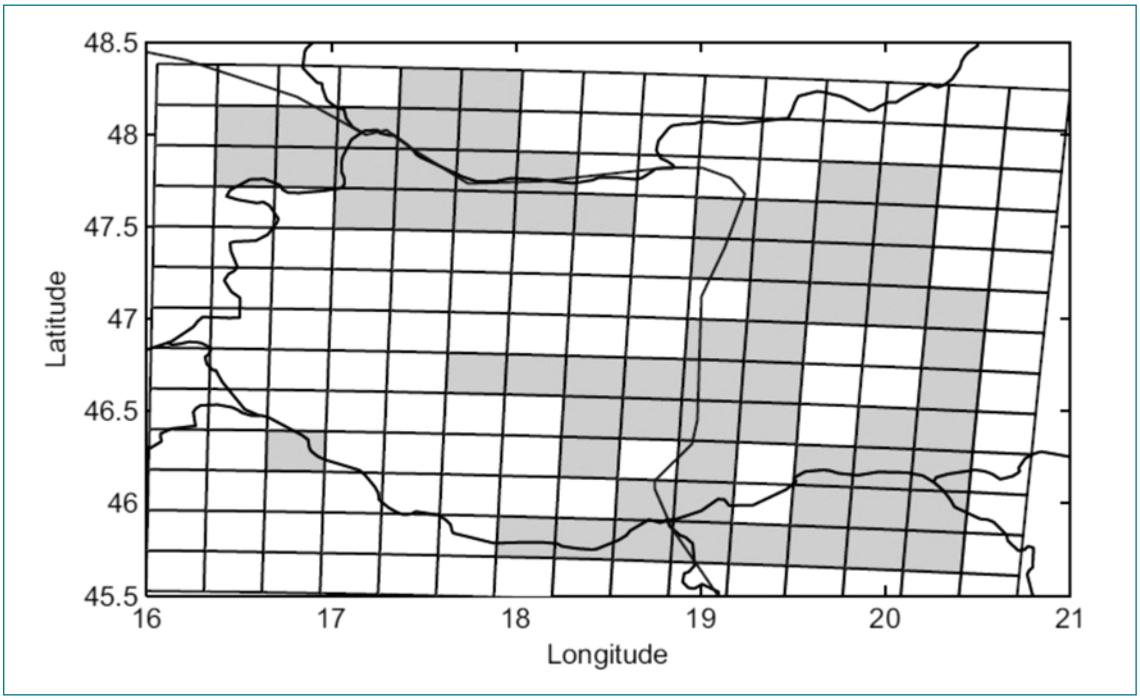

Figure 16.
(top) Soil depth classes and (bottom) groundwater affected soils (dark cells) occurring in the test region, as based on FAO soil classification and expected rooting depth and aggregated to the spatial resolution of 0.25 °.

Table 8.
Evaluated combinations of proposed modifications to HTESSEL. Four cases were considered. The differences with respect to the reference HTESSEL are indicated in grey.

Case	Reference	1	2	3	4
f_2 dependency	θ	ψ	θ	θ	ψ
Soil depth	2.89 m	2.89 m	variable	2.89 m	variable
Groundwater effect	no	no	no	yes	yes
N compartments	4	8	8	8	8

Table 9.
Summary statistics of the calculated evaporative fractions $\lambda E / R_n$ for the evaluated cases 1 to 4.

Case	Reference		1		2		3		4	
Initial condition	1	2	1	2	1	2	1	2	1	2
Mean $\lambda E / R_n$	0.62	0.62	0.7	0.69	0.60	0.60	0.62	0.63	0.67	0.66
10%-ile $\lambda E / R_n$	0.53	0.54	0.58	0.58	0.51	0.51	0.53	0.54	0.55	0.54
90%-ile$\lambda E / R_n$	0.70	0.71	0.79	0.80	0.70	0.71	0.71	0.71	0.79	0.78
RMSE(1) of $\lambda E / R_n$	0.06	0.06	0.09	0.08	0.07	0.07	0.06	0.05	0.08	0.08
R^2 of $\lambda E / R_n$	0.58	0.69	0.48	0.64	0.64	0.70	0.56	0.68	0.54	0.66

(1) Root Mean Square Error between model results and SEBAL data

Statistical properties of the calculated evaporative fractions are given in Table 9 for each case. Also the correlation coefficients between SEBAL and HTESSEL evaporative fraction are given.

For Case 1 the mean $\lambda E / R_n$ and variance increase with respect to the reference HTESSEL for Set 1 as well as Set 2. The increase of $\lambda E / R_n$, is consistent with the new f2 function that shows less root water uptake reduction for similar ψ and thus increased evaporation. However, the $\lambda E / R_n$ is too high compared to SEBAL $\lambda E / R_n$ and the RMSE is therefore larger than for the reference HTESSEL.

For Case 2 the mean evaporation decreases and the 10 percentile decreases as well as compared to the reference HTESSEL. The decreased evaporation is due to decreased moisture storage capacity for soil depths less than 2.89 m, i.e. in shallow soils the soil water is depleted more easily. Although additional spatial soil information is added, it only results in slightly increased variability of the calculated evaporation.

In Case 3 little improvement can be observed compared to the reference HTESSEL. The statistical properties of Case 3 are similar to that of the reference runs. We may thus conclude that to increase E the chosen parameterization does not increase the available water significantly.

For Case 4, the parameterization of Case 1 and Case 3 (increase of $\lambda E / R_n$) are expected to balance the effect of Case 2 (decrease of $\lambda E / R_n$). However, the effect of the new f_2 function appears to dominate the effect of the reduced soil depth. In particular this can be observed for larger $\lambda E / R_n$(see the 90^{th} percentiles).

For all cases the correlation between the calculated evaporative fraction and that of SEBAL was less than the reference case, except for Case 2 and the initial condition Set 1 of Case 1, which indicates that the model skill of HTESSEL to reproduce the spatially variable evaporation has not significantly been improved by the modifications.

5.7 General discussions and conclusions

The primary objective of this study is to assess the model skill of the land surface scheme HTESSEL to reproduce spatial patterns of surface evaporation in response to patterns in precipitation and land surface characteristics, with emphasis on the mean and spatial variability during dry (summer) periods. The secondary goal is to assess the effect of a number of model modifications.

The evaluation shows that, within the test region, HTESSEL predicts the seasonal energy partitioning of the incoming radiation over latent and sensible heat flux densities reasonable well, given the spatial and temporal resolution and the considered year 2005. The statistical properties of the seasonal evaporative fraction $\lambda E / R_n$ of HTESSEL and SEBAL are of the same magnitude, however, HTESSEL slightly underestimates $\lambda E / R_n$, especially for grid cells with low $\lambda E / R_n$. The RSME of HTESSEL is approximately twice the accuracy of SEBAL. The prediction error of the individual grid cells is up to 30% of the SEBAL $\lambda E / R_n$. The correlation coefficient of the calculated evaporative fraction to SEBAL evaporative fraction is between 0.58 and 0.69, dependent on the initial conditions used.

These results are based on atmospheric forcing of which the accuracy is unknown. Especially precipitation *P* may have a large impact on the calculated evaporation *E* (see also Figure 11) and a slight change in precipitation may change the calculated evaporative fractions. Longer evaluation periods are needed to confirm the observations.

The importance of representing correctly initial terrestrial water storages such as soil water and snow cover for modulating wet and dry meteorological anomalies is illustrated in Figure 14, which shows yearly precipitation *P* plotted against seasonal evaporation *E* of each individual grid cell. *E* of Set 1 has a scattered relationship to *P*, whereas Set 2 shows a largely linear relationship. Due to the cycling over 2005, the initial state of Set 2 reflects only the signature of the atmospheric forcing over 2005, which is dominated by *P* in the region considered. Instead, in Set 1 the initial water stored in the soil and snow pack reflects the signal of longer-term meteorological conditions, which is more realistic. In grid cells with low precipitation over 2005, the effect on $\lambda E / R_n$ may be moderated by the relatively wet soil moisture conditions originating from a previous (winter) period. The overall effect is a more scattered relationship between *P* en *E*.

Although longer evaluation periods are needed to confirm the results, the simulations performed with HTESSEL reveal a relatively low ability of the model to correctly predict E in areas where $P- E < 0$. Since the low precipitation areas coincide with irrigated areas, the underestimation of $\lambda E / R_n$ in grid cells with $(P - E) < 0$, might also point towards enhanced evaporation due to irrigated cropland. HTESSEL does neither incorporate the effect of irrigation, nor the effect of shallow groundwater on the water balance. Especially, during periods with high temperatures and low humidity, additional evaporation is expected due to the availability of irrigation and groundwater. Like other Land Surface Schemes (LSS), HTESSEL does not allow for lateral redistribution of precipitation due to surface and subsurface flow. LSSs are now being modified to include lateral flow, groundwater flow and surface water (e.g. Fan *et al.*, 2007; Miguez-Macho *et al.*, 2007), however these developments are still in an experimental stage. This is largely due to encountered difficulties to obtain the required hydrological data that needs global coverage and a correct resolution. By bridging the gap between hydrological and climate models and thus by incorporating lateral flow, including groundwater flow, irrigation and river routing, LSS skills may significantly improve.

Based on earlier sensitivity analysis of soil hydrologic processes (Metselaar *et al.*, 2006) we (i) revised the parameterization of the reduction of evaporation for dry vegetation, (ii) replaced the fixed soil depth with more realistic and variable soil depths, and (iii) introduced additional water availability due to capillary rise from shallow water tables. These modifications lead to increased spatial variability of soil hydrological processes, but they did not lead to significant improvement. (i) increased the $\lambda E / R_n$ too much, especially for grid cells in the higher $\lambda E / R_n$ range, (ii) decreased on $\lambda E / R_n$ (especially in the lower range) and increased the RMSE. The unrealistically large soil thickness in HTESSEL seems to compensate for the strong reduction of root water uptake under dry conditions. At higher spatial resolutions the spatial variability of soil and vegetation characteristics may become more important and a more physically based description of soil moisture movement may be warranted. Additional water availability (iii) did not lead to significant changes in $\lambda E / R_n$. A more rigorous parameterization for the groundwater dynamics may be needed to improve the models ability of predicting evaporative fractions in regions affected by shallow groundwater.

5.8 Summary

The skill of the land surface model HTESSEL has been assessed to reproduce evaporation in response to land surface characteristics and atmospheric forcing, both being spatially variable. Evaporation estimates for the 2005 growing season were obtained from satellite observations of the Western part of Hungary and compared to model outcomes. Atmospheric forcing was obtained from a hind cast run with the Regional Climate Model RACMO. Although HTESSEL slightly underestimated the seasonal evaporative fraction as compared to satellite estimates, the mean, 10th and 90th percentile of this variable were of the same magnitude as the satellite observations. The initial water as stored in the soil and snow layer did not have a significant effect on the statistical properties of the evaporative fraction. However, the spatial distribution of the initial soil and snow water affected significantly the spatial distribution of the calculated evaporative fraction and the models ability to reproduce evaporation correctly in low precipitation areas in the considered region. HTESSEL's performance appears to be less in dryer areas. In Western Hungary these areas are situated in the Danube valley, which is partly covered by irrigated cropland and which also may be affected by shallow groundwater. Incorporating (lateral) groundwater flow and irrigation, processes that are not included now, may improve HTESSEL's ability to predict evaporation correctly. Evaluation of the model skills using other test areas and larger evaluation periods is needed to confirm the results.

Based on earlier sensitivity analysis, the effect of a number of modifications to HTESSEL was assessed. A more physically based reduction function for dry soils was introduced, the soil depth was made variable and the effect of shallow groundwater included. However, for the case invesigated the modification did not lead to significant improved performance of HTESSEL.

6. Synthesis

The research activities described in the preceding chapters have been performed in the years 2005 – 2008. In this Synthesis Chapter we will consider most recent scientific literature with respect to improvement of land surface schemes in climate models and highlight the contribution of our research findings in this literature context. The following items are considered:

- relevance of soil moisture characteristics;
- performance of the current HTESSEL land surface scheme;
- inclusion of groundwater;
- inclusion of irrigation water;
- availability of input and verification data.

Relevance of soil moisture

Land energy and water balances are coupled through the evapotranspiration term. As soil moisture has a large impact on the energy partitioning at the land surface, it has a key role for both the water and energy cycle (Seneviratne *et al.*, 2010). Studies show that processes acting at the interface between the land surface and the atmosphere have a strong impact on the European summer climate, particularly during extreme years. Fischer *et al.* (2007b) explored the role of land surface–related processes during the record-breaking 2003 European summer heat wave with a regional climate model. A large precipitation deficit together with early vegetation green-up and strong positive radiative anomalies in the months preceding the extreme summer event contributed to an early and rapid loss of soil moisture, which exceeded the multiyear average by far. In this experiment the hottest phase in early August was realistically simulated despite the absence of an anomaly in total surface net radiation. This indicates an important role of the partitioning of net radiation in latent and sensible heat fluxes, which is to a large extent controlled by soil moisture. The lack of soil moisture strongly reduced latent cooling and thereby amplified the surface temperature anomalies. The evaluation of the experiments with perturbed spring soil moisture shows that this quantity is an important parameter for the evolution of European heat waves. Simulations indicate that without soil moisture anomalies the summer heat anomalies could have been reduced by around 40% in some regions (Fischer *et al.*, 2007b).

More recently, Jaeger and Seneviratne (2010) investigated the role of soil moisture–atmosphere coupling for the European summer climate over the period 1959–2006 using simulations with a regional climate model. The study focus was temperature and precipitation extremes and trends. Soil moisture – climate interactions were found to have significant effects on temperature extremes in the experiments, and impacts on precipitation extremes were also identified (Jaeger and Seneviratne, 2010).

In our study we ranked the importance of vegetation and soil factors, using a simulation experiment with the ecohydrological SWAP model. In this experiment the main water balance effects of individual factors were derived given simultaneous variation in all other factors. The ranking of the variables in terms of their relative effect suggests a priority in the processes to be incorporated in new climate land routines. Based on expert judgment, 13 factors were investigated: leaf area index and its time course, rooting depth and its time course, profile discretisation, analytical function of the soil hydraulic properties, stoniness, transpiration reduction function with respect to soil moisture, critical soil water pressure head, and lower boundary condition of the soil. Results show that choice of the lower boundary condition, rooting depth, and temporal course of leaf area index have the strongest effect on yearly and monthly evapotranspiration.

Performance of HTESSEL

Individual land surface models do show a wide range of sensitivity to soil moisture, both with respect to precipitation and evapotranspiration (Seneviratne *et al.*, 2010). Balsomo *et al.* (2009) tested the HTESSEL landroutine of regional climate model RACMO and compared model results against observations from field site experiments. The revision was introduced to correct two main shortcomings of the TESSEL land surface scheme: the absence of surface runoff and a globally uniform soil texture. A new dataset for soil type was included by assigning a hydrological class (up to six) to each grid cell. A revised infiltration scheme with a subgrid surface runoff description was also introduced and evaluated (Balsomo *et al.*, 2009).

In point comparisons with field site experiments, these modifications showed a shift in the soil moisture range to give better agreement with observations. The soil physiographic parameters (wilting point and field capacity) associated with each soil texture produced a larger water holding capacity. In dry regions, the shift of the soil moisture range gave slightly better evaporation. A set of regional stand-alone experiments was used to evaluate the terrestrial water storage variations over the central European river basins in comparison with independent estimates based on atmospheric moisture convergence data and river discharge observations. The model global annual runoff map showed some small improvement when compared with the river discharge product. Quantitative evaluation of the runoff at monthly time scales showed a net improvement of runoff timing in relevant catchments. In basins dominated by snow, spring snowmelt was still too early because of errors in the snow scheme. The annual bias in runoff was reduced for most of the basins considered (Balsomo *et al.*, 2009).

In our study, we investigated the skill of HTESSEL to reproduce spatial gradients of surface evaporation in response to gradients in precipitation and land surface characteristics. We obtained satellite evapotranspiration data for the 2005 growing season in the Western part of Hungary and compared these to HTESSEL model results. Atmospheric forcing was obtained from a hind cast run with the regional climate model RACMO. Although HTESSEL slightly underestimated the seasonal evaporative fraction as compared to satellite estimates, the mean, 10^{th} and 90^{th} percentile of this variable were of the same magnitude as the satellite observations. The initial water as stored in the soil and snow layer did not have a significant effect on the statistical properties of the evaporative fraction. However, the spatial distribution of the initial soil and snow water affected significantly the spatial distribution of the calculated evaporative fraction and the models ability to reproduce evaporation correctly in low precipitation areas in the considered region. HTESSEL's performance appears to be less in dry areas. In Western Hungary these areas are situated in the Danube valley, which is partly covered by irrigated cropland and which also may be affected by shallow groundwater. Incorporating (lateral) groundwater flow and irrigation, processes that are not included now, may improve HTESSEL's ability to predict evaporation correctly.

For the same area and period, we evaluated the effect of a number of modifications to HTESSEL: a more physically based root water uptake reduction function for dry soils, variable soil depth and a modification of the soil moisture characteristic to mimic impeded drainage and capillary rise from a shallow groundwater table. These modifications did not lead to a better performance of HTESSEL. The more physically based root water uptake reduction function increased the evapotranspiration too much, the decreased soil depth resulted in too low evapotranspiration, and the modification of the soil moisture characteristic was insufficient to explain the larger evapotranspiration in areas with shallow groundwater levels. Integrated model runs on European scale for larger time frames should reveal the real merit of these modifications.

Inclusion of groundwater

Subsurface flow is an important hydrologic process and a key component of the water budget. Through its direct impacts on soil moisture, it can affect water and energy fluxes at the land surface and influence the regional climate and water cycle. Huang *et al.* (2008) developed a new subsurface flow formulation that incorporates the spatial variability of both topography and recharge. The subsurface flows calculated using power-law and exponential parameterizations compared well with values derived from observations at Tulpehocken Creek, Pennsylvania, and Walnut Creek, Iowa. An important conclusion of this study is that the spatial variability of recharge alone, and/or in combination with the spatial variability of topography can substantially alter the behaviours of subsurface flows. This suggests that in macroscale hydrologic models or land surface models, subgrid variations of recharge and topography can make significant contributions to the grid mean subsurface flow and must be accounted for in regions with large surface heterogeneity. This is particularly true for regions with humid climate and a relatively shallow groundwater table where the combined impacts of spatial variability of recharge and topography are shown to be more important. For regions with an arid climate and a relatively deep groundwater table, simpler formulations, for example, the power law, for subsurface flow can work well, and the impacts of subgrid variations of recharge and topography may be ignored (Huang *et al.*, 2008).

Fan *et al.* (2007) used USGS observations to examine the spatial and temporal characteristics of water table depth in the lower 48 states of the United States. They found that, at many sites in the eastern part of the country, as well as in closed basins and mountainous valleys in the West, the water table is shallow, lying within 5 m of the land surface. Thus there is a potential for the water table to anchor the soil moisture patterns in these regions. Temporally, they observed a strong seasonal cycle and significant interannual variability, at most sites. In addition, upward and downward fluctuations in water table depth at event and diurnal timescales reflected the balance between vertical drainage, lateral subsurface flow to local streams, and the upward flux to feed evapotranspiration. The longer time scales of the lateral processes, as well as the inertia provided by the large groundwater reservoir, have a potential for increasing soil moisture memory. While providing the best available direct observational coverage, water table observations are still scattered and sparse in most areas. Fan *et al.* (2007) used a simple two-dimensional groundwater flow model, constrained by the USGS observations, to construct an equilibrium water table as a means for synthesizing and interpolating between the measurements.

In this study we formulated a drainage concept which uses two key parameters: the drainage resistance and the drainage level. Such a concept should be able to capture both the impeded drainage and the capillary rise at shallow groundwater levels. The main challenge is to make maps with values of drainage resistance and drainage level which are representative for the spatial scale of regional climate models. The pixel values of drainage resistance and drainage level might be derived by inverse modeling, using the FAO-drainage classification or national classifications, such as the Dutch drainage classes, as resource.

Inclusion of irrigation water

Lobell *et al.* (2009) performed a global climate model experiment to evaluate the effect of irrigation on temperatures in several major irrigated regions of the world. The Community Atmosphere Model was modified to represent irrigation for the fraction of each grid cell equipped for irrigation according to datasets from the FAO. Irrigation was applied as soon as the actual soil moisture content fell below a specified critical soil moisture level. Results indicate substantial regional differences in the magnitude of irrigation-induced cooling, which are attributed to three primary factors: differences in extent of the irrigated area, differences in the simulated soil moisture, and the nature of cloud response to irrigation. The last factor appeared especially important for the dry season in India, although further analysis with other models and observations are needed to verify this feedback. Comparison with observed temperatures revealed substantially lower temperature biases in several regions for the simulation with irrigation (Lobell et al., 2009).

Using the Regional Atmospheric Modeling System, Douglas *et al.* (2009) show that agricultural intensification and irrigation modifies the surface moisture and energy distribution, which alters the boundary layer and regional convergence, mesoscale convection, and precipitation patterns over the Indian monsoon region. Results indicate that even under active monsoon conditions, the simulated surface energy and moisture flux over the Indian monsoon region are sensitive to the irrigation intensity and this effect is more pronounced than the impact of land use change from the potential vegetation to the agricultural landscape. Irrigation increased the regional moisture flux which in turn modified the convective available potential energy. This caused a reduction in the surface temperature and led to a modified regional circulation pattern and changes in mesoscale precipitation. These agricultural changes, including irrigation, modify the mesoscale convection and rain patterns in the Indian monsoon region (Douglas *et al*., 2009).

In our study in Hungary, we encountered too low simulated actual evapotranspiration with HTESSEL which does not account for irrigation, in areas which are known to be irrigated. Incorporation of irrigation will decrease the noticed temperature bias in this area. A concept such as used by Lobell *et al.* (2009) might be worth to consider for HTESSEL.

Availability of input and verification data

Despite strong increase in complexity of the available land surface models, even simple relationships and parameters are still unknown. For instance, the water holding capacity, which is recognized as one of the key variables for soil moisture – climate relationships, is highly variable between state of the art global climate models (Seneviratne *et al*., 2006). The requirements for better soil hydraulic data were illustrated by a study of Dutra *et al.* (2008) with the land routine TESSEL for the drought prone Iberian peninsula. They showed that, although the spatial heterogeneity of precipitation is the main driver of the spatial variability of drought, the spatial distribution of soil characteristics modulates its temporal variability.

Also a recent study by Horváth *et al.* (2009) shows the importance of correct soil hydraulic parameters. In their study the effect of the soil hydraulic functions on the prediction of storm fields was as large as the parameterization of the stomatal resistance. They advocate that regional climate models should use local soil data bases instead of global soil data bases. Anders and Rockel (2009) performed regional climate simulations with different prescribed soil type distributions to investigate consistent dry and warm biases during summer in south-eastern Europe. The conventional soil type distribution defines sandy loam in the southeast of Europe; whereas the modified one defines a large area of silt loam instead. As a consequence of the different soil characteristics, the results indicated increased soil moisture in the modified simulation compared to the control simulation. In addition to local changes in near surface parameters, large-scale changes involving temperature, precipitation and surface pressure were observed. Some corrections of the temperature bias in south-eastern Europe were obtained with the prescription of the different soil type, though significant model biases remained in this region.

In our study we show that in Europe considerable scope exists for adding relevant soil information. The following physical factors may be added: soil depth, soil salinity, soil texture, soil stoniness and groundwater levels. Soil depth, soil salinity, soil texture and soil stoniness are part of the WISE database. The soil texture data can be used to generate more accurate soil moisture retention and hydraulic conductivity functions, using the HYPRES pedotransfer functions.

Verification of regional climate model results is hampered by differences in scale between models and observations. Common ground measurements of soil moisture include gravimetric, time domain reflectrometry, neutron probes, electric resistance and fiber optic sensors. These measurements may have a high time resolution, but their spatial resolution is much smaller than those of regional climate models. Satellite remote sensing observations (e.g. microwave remote sensing), on the other hand, cover large areas, but have a low time resolution (Seneviratne *et al.,* 2010). A remaining key challenge is to continue to develop ground-based monitoring networks for soil moisture and evapotranspiration. Several efforts have been initiated in this direction: for example, the soil moisture measurements of the Oklahoma Mesonet (Basara and Crawford, 2000), the REMEDHUS network (Martinez-Fernandez and Ceballos, 2003), the AMMA project

(Redelsperger *et al.*, 2006), the SMOSREX ground-measurement experiment (De Rosnay *et al.*, 2006), the NAFE campaign (Panciera *et al.*, 2008), as well as the new TERENO, SwissSMEX, and ICOS initiatives.

In our study we showed the value of satellite evapotranspiration data to evaluate the performance of RCM land routines. We used data of the MODIS satellite with a spatial resolution of 1 km, and applied the SEBAL algorithm. The satellite data revealed in which particular areas at the scale of regional climate models the HTESSEL landroutine over- and underestimated evapotranspiration fluxes. This is very usefull for further development of current landroutines.

References

Anders, I. & B. Rockel, 2009. The influence of prescribed soil type distribution on the representation of present climate in a regional climate model. Climate Dynamics, 33, 177-186.

Balsamo, G., P. Viterbo, A.Beljaars, B. van den Hurk, M. Hirschi, A.K. Betts & K. Scipal, 2009. A revised hydrology for the ECMWF model: Verification from field site to terrestrial water storage and impact in the Integrated Forecast System. Journal of Hydrometeorology, 10, 623-643.

Basara, J.B. & T.M. Crawford, 2000. Improved installation procedures for deep-layer soil moisture measurements. Journal of Atmospheric and Oceanic Technology, 17, 879–884.

Bastiaanssen, W.G.M., 2000: SEBAL-based sensible and latent heat fluxes in the irrigated Gediz Basin, Turkey. Journal of Hydrology, 229, 87-100.

Bastiaanssen, W.G.M., M. Menenti, R.A. Feddes & A.A.M. Holtslag, 1998. The Surface Energy Balance for Land (SEBAL): Part 1 formulation. Journal of Hydrology, 212-213, 198-212.

Bastiaanssen, W.G.M., E.J.M. Noordman, H. Pelgrum, G. Davids, B.P. Thoreson & R.G. Allen, 2005: SEBAL model with remotely sensed data to improve water-resources management under actual field conditions. ASCE Journal of Irrigation and Drainage Engineering, 131, 85-93.

Batjes, N.H., 2002a. A homogenized soil profile data set for global and regional environmental research (WISE, version 1.1). Report 2002/01. International Soil Reference and Information Centre, Wageningen. Available at www.isric.org.

Batjes, N.H., 2002b. Soil parameter estimates for the soil types of the world for use in global and regional modelling (WISE, version 2.1). ISRIC report 2002/02c. International Soil Reference and Information Centre, Wageningen. Available at www.isric.org.

Beck, M.B. 1987. Water quality modeling: a review of the analysis of uncertainty. Water Resources Research, 23, 1393-1442.

Betts, A.K., J.H. Ball, A.C.M. Beljaars, M.J.Miller & P.A. Viterbo, 1996. The land surface-atmosphere interaction: A review based on observational and global modeling perspectives. Journal of Geophysical Research, 101, 7209-7225.

Choudhury, B. J., 1997. Global pattern of potential evaporation calculated from the Penman-Monteith equation using satellite and assimilated data. Remote Sensing of Environment, 61, 64–81.

Choudhury, B. J., & N. E. DiGirolamo, 1998. A biophysical process-based estimate of global land surface evaporation using satellite and ancillary data. I. Model description and comparison with observations. Journal of Hydrology, 205, 164–185.

De Bruin, H.A.R. & J.N.M. Stricker, 2000. Evaporation of grass under non-restricted soil moisture conditions. Hydrological Sciences Journal, 45, 391-406.

De Rosnay, P., et al., 2006. SMOSREX: a long term field campaign experiment for soil moisture and land surface processes remote sensing. Remote Sensing of Environment, 102, 377–389.

de Wit, C.T, R. Brouwer, F.W.T & Penning de Vries, 1970. The simulation of photosynthetic systems. Page 47-70 in: I. Setlik (ed.) prediction and measurement of photosynthetic productivity: Proceedings of the IBP-PP technical meeting Trebon. Wageningen: PUDOC.

Douglas, E.M., Beltrán-Przekurat, A., Niyogi, D., Pielke Sr., R.A. & Vörösmarty, C.J., 2009. The impact of agricultural intensification and irrigation on land-atmosphere interactions and Indian monsoon precipitation - A mesoscale modeling perspective. Global and Planetary Change, 67, 117-128.

Dümenil, L. & E. Todini, 1992. A rainfall-runoff scheme for use in the Hamburg climate model. Advances in Theoretical Hydrology, a tribute to James Dooge. P. O'Kane (ed.), European Geophysical Soc. Series on Hydrological Sciences 1, Elsevier, Amsterdam.

Dutra, E., P. Viterbo & P.M.A. Miranda, 2008. ERA-40 reanalysis hydrological applications in the characterization of regional drought. Geophysical Research Letters, 35, L19402.

ECMWF, 2006. Site http://www.ecmwf.int/research/ifsdocs/

ECMWF, 2007: ECMWF Documentation Cycle CY28r1, part 4: Physical processes, Chapt. 7: Surface parameterization. Available at http://www.ecmwf.int/research/ifsdocs/CY31r1/PHYSICS/

Eusoils, 2006a. Site http://eusoils.jrc.it/

Eusoils, 2006b. Site http://eusoils.jrc.it/ESDB_Archive/groundwater/gw.html

Fan, Y., G. Miguez-Macho, C. P. Weaver, R. Walko & A. Robock, 2007. Incorporating water table dynamics in climate modeling : 1. Water table observations and equilibrium water table simulations. Journal of Geophysical Research, 112, D10125.

FAO, 1995: Digital soil map of the world and derived soil properties. Version 3.5. Food and Agriculture Organization of the United Nations, Rome, Italy.

Feddes, R.A., and P.A.C. Raats. 2004. Parameterizing the soil-water-plant root system, p. 95–141. In R.A. Feddes et al. (ed.) Unsaturated-zone modeling: Progress, challenges and applications. Wageningen UR Frontis Series. Kluwer Academic Publishers, Dordrecht, The Netherlands.

Fischer, G., H. van Velthuizen & F. O. Nachtergaele (2000). Global Agro-Ecological Zones Assessment: Methodology and Results. Interim Report IR-00-064, IIASA, Laxenburg.

Fischer, E. M., S. I. Seneviratne, D. Lüthi & C. Schär, 2007a. Contribution of land-atmosphere coupling to recent European summer heat waves. Geophysical Research Letters, 34, L06707, doi:10.1029/2006GL029068.

Fischer, E.M., S.I. Seneviratne, P.L. Vidale, D. Lüthi, & C. Schär, 2007b. Soil moisture-atmosphere interactions during the 2003 European summer heat wave. Journal of Climate, 20, 5081-5099.

Fraters, D. 1996. Generalized soil map of Europe: Aggregation of the FAO-Unesco soil units based on the characteristics determining the vulnerability to soil degradation processes. Report 481505006, RIVM, Bilthoven, The Netherlands.

GenStat Committee (2003). GenStat® Release 7.1 Reference Manual Part 2: Directives VSN Int., Oxford.

Gerwitz, A. & E.R. Page, 1974. An empirical model to describe plant root systems. Journal of Applied Ecology, 11, 773-781.

Hagemann, S., B. Machenhauer, R. Jones, O.B. Christensen, M. Déqué, D. Jacob & P.L Vidale, 2004. Evaluation of water and energy budgets in regional climate models applied over Europe. Climate Dynamics, 23, 547-567.

Hollis, J.M., I.P. Holman, R.G.O. Burton, C.M. Willers & D. Pavelley, 2002. A digital dataset of European groundwater resources at 1:500,000. (v1.0). Available at
http://eusoils.jrc.it/ESDB_Archive/groundwater/docs/EUGWFR.pdf

Hirschi, M., S. Seneviratne, & C. Schär, 2006. Seasonal variations in terrestrial water storage for major mid-latitude river basins. Journal of Hydrometrology, 7, 39-60.

Horváth, Á., F. Ács & H. Breuer, 2009. On the relationship between soil, vegetation and severe convective storms: Hungarian case studies. Atmospheric Research, 93, 66-81.

Huang, M., X. Liang, L.R. Leung, 2008. A generalized subsurface flow parameterization considering subgrid spatial variability of recharge and topography. Journal of Hydrometeorology, 9, 1151-1171.

Hypres, 2006. Site http://www.macaulay.ac.uk/hypres/index.html

Jackson, R.B., J. Canadell, J.R. Ehleringer, H.A. Mooney, O.E. Sala & E.D. Schulze, 1996. A global analysis of root distributions for terrestrial biomes. Oecologia, 108, 389-411

Jaeger, E.B. & S.I. Seneviratne, 2010. Impact of soil moisture-atmosphere coupling on European climate extremes and trends in a regional climate model. Climate Dynamics, in press.

Jarvis, P.G., 1976. The interpretation of the variations in leaf water potential and stomatal conductance found in canopies in the field. Philosophical transactions of the Royal Society of London series B-Biological Sciences, 273, 593-610.

Kleijnen, J.P.C., 1987. Too many factors: screening. Chapter 28 in: Statistical tools for simulation practitioners. Statistics: textbooks and monographs vol. 76. New York: Marcel Dekker.

Kroes, J.G., J.C. van Dam, P. Groenendijk, R.F.A. Hendriks & C.M.J. Jacobs, 2008. SWAP version 3.2. Theory description and user manual. Alterra report 1649. Alterra, Wageningen.

Lenderink, G, B. van den Hurk, E. van Meijgaard, A. van Ulden & H. Cuijpers, 2003. Simulation of present-day climate in RACMO2: First results and model developments, KNMI Tech. Report 252.

Leff, B., N. Ramankutty & J. A. Foley, 2004. Geographic distribution of major crops across the world. Global Biogeochemical cycles, GB1009.

Lobell, D., G. Bala, A. Mirin, T. Phillips, R. Maxwell * D. Rotman, 2009. Regional differences in the influence of irrigation on climate. Journal of Climate, 22, 2248-2255.

Martinez-Fernandez, J. & A. Ceballos, 2003. Temporal stability of soil moisture in a large field experiment in Spain. Soil Science Society of America Journal, 67, 1647–1656.

Masson, V., J-L. Champeaux, F. Chauvin, C. Meriquet & R. Lacaze, 2003. A Global database of land surface parameters at 1-km resolution in meteorological and climate models. Journal of Climate, 16, 1261-1282.

Metselaar K., J.C. van Dam & R. A. Feddes, 2006a. Screening and understanding the importance of soil hydrology related factors in a SVAT scheme. Part 1: Screening factors to establish the relative importance. Part 2: A study of numerical discretization, rooting depth, and bottom boundary condition. Reports in the Framework of the KvR project CS3.

Metselaar K., R.A. Feddes & J.C. van Dam, 2006b. Soil variability in Europe, and a quick scan of its parameterization for use in SVAT-schemes. Reports in the Framework of the KvR project CS3.

Metselaar K., V.L. Versace, R.A. Feddes & J.C. van Dam, 2006c. Root depth distributions. Part 1: Root depth distributions of important agricultural crops. Part 2: Root depth distributions of vegetation types – a reclassification. Reports in the Framework of the KvR project CS3.

Miguez-Macho, G., Y. Fan, C.P. Weaver, R.Walko & A. Robock, 2007. Incorporating water table dynamics in climate modeling: 2. Formulation, validation, and soil moisture simulation. Journal of Geophysical Research, 112, D13108 .

Nemes, A., M.G. Schaap & J.H.M. Wösten, 2003. Functional evaluation of pedotransfer functions derived from different scales of data collection. Soil Science Society of America Journal, 67, 1093-1102

Van Noordwijk, M. & S.C. van de Geijn, 1996. Root, shoot and soil parameters required for process-oriented models of crop growth limited by water or nutrients. Plant and Soil, 1996, 183, 1-25.

O'Toole, J.C. & W.L. Bland, 1987. Genotypic variation in crop plant root systems. Advances in Agronomy, 85, 181-219.

Panciera, R. & et al., 2008. The NAFE'05/CoSMOS data set: toward SMOS soil moisture retrieval, downscaling, and assimilation. IEEE T. Geoscience Remote, 46, 736–745.

PILPS, 2006. Site http://gaim.unh.edu/Structure/Future/MIPs/PILPS.html

Redelsperger, J.L., C.D. Thorncroft, A. Diedhiou, T. Lebel, D.J. Parker & J. Polcher, 2006. African monsoon multidisciplinary analysis—an international research project and field campaign. Bulletin American Meteorological Society, 87, 1739–1746.

Reynolds, C. A., T.J. Jackson & W.J. Rawls, 2000. Estimating soil water-holding capacities by linking the Food and Agriculture Organization Soil Map of the World with global pedon databases and continuous pedotransfer functions. Water Resources Research, 36, 3653-3662.

Saxton, K., W. Rawls, J. Romberger & R. Papendick, 1986. Estimating generalized soil water characteristics from texture. Soil Science Society of America Journal, 50, 1031-1036.

Schenk, H.J. & R.B. Jackson, 2002. The global biogeography of roots. Ecological monographs, 72, 311-328.

Seneviratne, S.I, P.Viterbo, D. Lüthi & C. Schär, 2004. Inferring changes in terrestrial water storage using ERA-40 reanalysis data: The Mississippi River basin. Journal of Climate, 17, 2039-2057.

Seneviratne, S.I., R.D. Koster, Z. Guo, P.A. Dirmeyer, E. Kowalczyk, D. Lawrence, P. Liu, C.-H Lu, D. Mocko, K.W. Oleson & D. Verseghy, 2006. Soil moisture memory in AGCM simulations: analysis of Global Land–Atmosphere Coupling Experiment (GLACE) data. Journal of Hydrometeorology, 7, 1090–1112.

Seneviratne, S.I., T. Corti, E.L. Davin, M. Hirschi, E.B. Jaeger, I. Lehner, B. Orlowsky & A.J. Teuling, 2010. Investigating soil moisture-climate interactions in a changing climate: A review. Earth-Science Reviews, 99, 125-161.

Siebert, S., P.Döll, S. Feick, J. Hoogeveen & K. Frenken, 2007. Global Map of Irrigation Areas version 4.0.1. Johann Wolfgang Goethe University, Frankfurt am Main, Germany / Food and Agriculture Organization, Rome, Italy.

Sinclair, T.R. & C.T. de Wit, 1976. Analysis of the carbon and nitrogen limitation to soybean yield. Agronomy Journal, 68, 319-324.

Stanners, D. & P. Bourdeau, 1995. Europe's Environment - The Dobris Assessment, State of Environment report No 1/1995. Luxembourg: Office for Official Publications of the European Communities, 676 p. Available at http://reports.eea.europa.eu/92-826-5409-5/en/tab_content_RLR

Szalia, S., Z. Bihari, M. Lakatos & T. Szentimrey, 2005. Some characteristics of the climate of Hungary since 1901. Hungaria Meteorological Service Report.

Tuba, Z., Z. Nagy & Z. Csintalan. 2005: CarboeuropeIP Ecosystem Component Database. Available at http://gaia.agraria.unitus.it/database

Uppala, S.M., et al., 2005. The ERA-40 re-analysis. Quarterly Journal of the Royal Meteorological Society, 131, 2961-3012.

Van Dam, O., J.W.M. van der Drift & C.A. van Diepen, 1994. Estimation of the Available Soil Moisture Capacity for the soil units of the EC soil map. DLO Winand Staring Centre, Wageningen, the Netherlands. Technical Document 20.

Van Dam, J.C., P. Groenendijk, R.F.A. Hendriks & J.G. Kroes, 2008. Advances of modeling water flow in variably saturated soils with SWAP. Vadose Zone Journal, 7, 640-653.

Van den Hurk, B. & P. Viterbo, 2003: The Torne-Kalix PILPS 2(e) experiment as a test bed for modifications to the ECMWF land surface scheme. Global and Planetary Change, 38, 165-173.

Van den Hurk, B.J.J.M., P. Graham & P. Viterbo, 2002. Comparison of land surface hydrology in regional climate simulations of the Baltic Sea catchment. Journal of Hydrology, 255, 169-193.

Van Meijgaard, E. , L.H. van Ulft, W.J. van de Berg, F.C. Bosveld, B.J.J.M. van den Hurk, G. Lenderink and A.P. Siebesma, 2008. The KNMI regional atmospheric climate model RACMO, version 2.1. KNMI Technical Report 302.

Viterbo, P., A. Beljaars, J.-F. Mahfouf & J. Teixeira, 1999. The representation of soil moisture freezing and its impact on the stable boundary layer. Quarterly Journal of the Royal Meteorological Society, 125, 2401-2426.

Voogt, M.P., 2006: Meteolook - a physically based regional distribution model for measured meteorological variables. M.Sc. thesis Delft University of Technology, Delft, The Netherlands.

Welch, W.J., R.J. Buck, J. Sacks, H.P. Wynn, T.J. Mitchell & M.D. Morris, 1992. Screening, predicting and computer experiments. Technometrics, 34, 15-25.

WRR, 1992. Crop production potential of rural areas within the European Communities. Working Documents I-V, Netherlands Scientific Council for Government Policy, The Hague.

Zeng, X., Y-J. Dai, R.E. Dickinson M. Shaikh, 1998. The role of root distribution for climate simulation over land. Geophysical Research Letters, 25, 4533-4536.

Zwart, S.J. & W.G.M. Bastiaanssen, 2007. SEBAL for detecting spatial variation of water productivity and scope for improvement in eight irrigated wheat systems. Agricultural Water Management, 89, 287-296.

Annex: Publication list KvR project CS3

Scientific papers

De Jong van Lier, Q., K. Metselaar & J. C. van Dam, 2006. Root Water Extraction and Limiting Soil Hydraulic Conditions Estimated by Numerical Simulation. Vadose Zone Journal, 5, 1264-1277.

Metselaar, K. & Q. de Jong van Lier, 2007. The Shape of the Transpiration Reduction Function under Plant Water Stress. Vadose Zone Journal, 6, 124-139.

De Jong van Lier, Q., J.C. van Dam, K. Metselaar, R. de Jong & W.H.M. Duijnisveld, 2008. Macroscopic root water uptake distribution using a matric flux potential approach. Vadose Zone Journal, 7, 1065-1078.

Wipfler, E.L, K. Metselaar, J.C. van Dam, R.A. Feddes, E. van Meijgaard, B. van Ulft, B. van den Hurk, S. Swart & W.G.M. Bastiaanssen, 2011. Seasonal evaluation of the ECMWF land surface scheme against remote sensing energy fluxes of the Transdanubian region in Hungary. Submitted to Hydrology and Earth System Sciences.

Proceedings

Metselaar K., J.C. van Dam, R.A. Feddes & V.L. Versace, 2006. Soil Parameters and Vegetation Types in a SVAT Scheme, and their relative Importance for modeling Water Balance Terms in Weather Forecast Models. Geophysical Research Abstracts, Vol. 8, 02915, 2006 SRef-ID: 1607-7962/gra/EGU06-A-02915.

Metselaar K. & R.A. Feddes, 2006. Profile der Wurzellängendichte für Anwendung in meteorologischen SVAT-Modellen und Folgen für den Wasserhaushalt. Pagina 47-55 in Langensiepen, M., ed. Modellierung pflanzlicher Systeme aus historischer und aktueller Sicht. Symposium zu Ehren von Prof. Dr. Dr. h. c. Eilhard Alfred Mitscherlich, Humboldt Universität Berlin, 2-3 Februari 2006.

Metselaar K., R.A. Feddes, & S.E.A.T.M. van der Zee, 2006. Importance of root depth distribution for modeling of the interactions between water, soil, vegetation and atmosphere International Conference Hydrology and Ecology: The Groundwater/Ecology Connection, 11–14 September 2006 Karlovy Vary, Czech Republic, to be published as IAHS-publication [CS3]

Scientific reports

Metselaar K., J.C. van Dam & R. A. Feddes, 2006a. Screening and understanding the importance of soil hydrology related factors in a SVAT scheme. Part 1: Screening factors to establish the relative importance. Part 2: A study of numerical discretization, rooting depth, and bottom boundary condition. Reports in the Framework of the KvR project CS3.

Metselaar K., R.A. Feddes & J.C. van Dam, 2006b. Soil variability in Europe, and a quick scan of its parameterization for use in SVAT-schemes. Reports in the Framework of the KvR project CS3.

Metselaar K., V.L. Versace, R.A. Feddes & J.C. van Dam, 2006c. Root depth distributions. Part 1: Root depth distributions of important agricultural crops. Part 2: Root depth distributions of vegetation types – a reclassification. Reports in the Framework of the KvR project CS3.

Posters and presentations

Metselaar K., 2006. Workshop International Soil Moisture Group, ESTEC, Noordwijk, The Netherlands, 28-29 March 2006.

K. Metselaar, J.C. van Dam, R.A. Feddes & L. Wipfler, 2008. Representation of soil moisture and root water uptake in climate model: “Soil water balance”. Symposium Klimaat voor Ruimte, September 2007, The Hague.

Wipfler, E.L., K. Metselaar, J.C. van Dam, R.A. Feddes, E. van Meijgaard, B.J.J.M. van den Hurk, S.J. Zwart & W.G.M. Bastiaansen, 2008. Testing of modifications in the land surface scheme HTESSEL. Meeting European Geophysical Union, 13-18 April 2008, Vienna.

Feddes, R.A., K. Metselaar, I Wipfler & J.C. van Dam, 2008. Soil-vegetation-atmosphere transfer in regional climate modeling. Workshop Wasser- und Stoffflüsse in der Landschaft : Messung und Modellierung zum Schutz von Boden und Wasser, Kiel, 29 May 2008.

Wipfler, E.L., 2008. Modification and testing of a land surface scheme as adopted by RCM RACMO. Meeting HydroPredict, 15-18 September, Prague.

Climate changes Spatial Planning

Climate change is one of the major environmental issues of this century. The Netherlands are expected to face climate change impacts on all land- and water related sectors. Therefore water management and spatial planning have to take climate change into account. The research programme 'Climate changes Spatial Planning', that ran from 2004 to 2011, aimed to create applied knowledge to support society to take the right decisions and measures to reduce the adverse impacts of climate change. It focused on enhancing joint learning between scientists and practitioners in the fields of spatial planning, nature, agriculture, and water- and flood risk management. Under the programme five themes were developed: climate scenarios; mitigation; adaptation; integration and communication. Of all scientific research projects synthesis reports were produced. This report is part of the Climate scenarios series.

Climate scenarios

The projects in this field are designed to obtain high quality climate information and scenarios relevant for the Netherlands. The projects both focus on an improved monitoring and modelling of regional climate variability, and at the construction of tailored climate change scenarios suitable for exploring spatial adaptation options, such as flood retention areas or coastal defense. In all fields special attention is devoted to extreme climate conditions. The climate scenarios are designed and developed jointly with a number of key stakeholders.

Programme Office Climate changes Spatial Planning

c/o VU University Amsterdam, FALW
De Boelelaan 1085
1081 HV Amsterdam
The Netherlands
T +31 20 598 7318
office@klimaatvoorruimte.nl

c/o Alterra, Wageningen UR
P.O. Box 47
6700 AA Wageningen
The Netherlands
T +31 317 48 6540
info@klimaatvoorruimte.nl

www.climatechangesspatialplanning.nl